Stony Brook University

Neuronal Activation with Gain Modification of the Trigeminal Blink Reflex

A Dissertation Presented

by

Patricia Enmore

to

The Graduate School

in Partial Fulfillment of the Requirements

for the Degree of

Doctor of Philosophy

in

Neuroscience

Stony Brook University

December 2016

(include this copyright page only if you are selecting copyright through ProQuest, which is optional)

Stony Brook University

The Graduate School

Patricia Enmore

We, the dissertation committee for the above candidate for the

Doctor of Philosophy degree, hereby recommend

acceptance of this dissertation.

L. Craig Evinger– PhD, Professor
Department of Neurobiology and Behavior
(Advisor)

Alfredo Fontanini – PhD,MD, Associate Professor
Department of Neurobiology and Behavior
(Defense Chairperson)

Dr. Mary Kritzer – PhD, Professor
Department of Neurobiology and Behavior

Dr. William Collins – PhD, Associate Professor
Department of Neurobiology and Behavior

John Robinson- PhD, Professor
Department of Psychology

This dissertation is accepted by the Graduate School

Charles Taber
Dean of the Graduate School

Abstract of the Dissertation

Neuronal Activation with Gain Modification of the Trigeminal Blink Reflex

by

Patricia Enmore

Doctor of Philosophy

in

Neuroscience

Stony Brook University

2016

The trigeminal blink reflex is a simple circuit for investigating the neural bases of motor plasticity in mammals. Stimulating the supraorbital branch of the trigeminal nerve (SO) evokes two bursts of activity in the lid closing orbicularis oculi muscle, R1 and R2. One procedure for inducing blink plasticity is high frequency stimulation (HFS) of the SO. Presenting HFS before the R2 component (HFS-B) reduces blink amplitude for at least one hour in humans and rats. This reduction in blink amplitude is a decrease in gain because the blink evoking stimulus is the same before and after HFS-B treatment.

To identify neurons in the trigeminal blink circuit that participate in this form of blink plasticity c-Fos immunohistochemistry was utilized. One group of rats underwent HFS-B treatment and a second control group received individual SO stimuli instead of HFS-B treatment. The data showed that the number of c-Fos labeled neurons in the trigeminal nucleus correlated inversely with the reduction in reflex blink gain. The cerebellum plays a major role in motor plasticity. To investigate whether the cerebellum participated in blink reflex plasticity, c-Fos labeling was measured in a cerebellar input nucleus, the inferior olive (IO) and the red nucleus, which receives an output from the cerebellum. As with the trigeminal complex, the number of c-Fos labeled cells in the IO and RN correlated inversely with the reduction in reflex blink gain.

The inverse relationship between the number of c-Fos labeled cells and the suppression of trigeminal reflex blink circuit activity suggests that circuit inhibition requires activating more cells than enhancing trigeminal blink circuit activity. These data are important in considering how pathological states modulate trigeminal reflex blink circuits.

I dedicate this thesis to my wonderful, amazing, intelligent children, my mother and Dennis Edwards Jr. Thank you for the daily motivation and your wonderful sense of humor.

Table of Contents

List of Figures/Tables/Illustrations

Acknowledgments

Alhamdulillah!!! I would like to thank God for giving me the strength to achieve this degree. Over the years I have faced many challenges, but his plan for me was bigger than the plan I had for myself. Special thank you to my parents, especially my mother for motivating, encouraging and praying daily for me. I love you dearly and words cannot express how much you mean to me. Thank you for your unconditional support. To my children, I love you. You inspired and reminded me to never quit - thank you for those days. Over the years you sacrificed many nights and days with me for this accomplishment. I am blessed to have you both in my life. My grandparents (late Aubrey Thompson) and Una Thompson, thank you for believing in me and loving me throughout the years. My brothers (Kester and Kerry) you remind me daily that I can achieve anything. I love you forever near or far.

I met a man 8 years ago who changed my life. He encouraged me to go back to school and become a doctor. He stood by me while I took on this great challenge. Everyday he made me laugh and reminded me to enjoy the moment. Dennis, my love, I'm forever grateful and blessed just to have you by my side.

To the Thompson family, Fally and Mr. Felix a special thank you for the motivation and great laughter when it was most needed. Along this journey, God has blessed me with the people I needed. To my friends Jennifer, Onika, Mala, Cam and Sneha, thank you for always encouraging me and believing in me when I didn't believe in myself. You were there throughout my tears and laughter. I appreciate every one of you and I will forever cherish our friendship. To members of Lodge Truth Church thank you for all your prayers throughout the years, may God bless all of you.

Special thank you to my advisor Dr. Craig Evinger, you are truly an inspiration and motivation. To my committee, thank you for making me think outside the box. Special thanks to Graduate Program Director Dr. Kritzer for making me feel important. A special thanks to the current and past lab members (Teba, Jamie and Mike) of the Evinger lab. To the CIE thank you for all the support.

Chapter 1

Introduction

Abnormalities in motor adaptation occur in many diseases. The nervous system constantly adapts, so that a given input to the motor system produces the appropriate movement. This modification of the motor system is called motor adaptation. Motor adaptation is impaired in Parkinson's disease (PD) [1] and in rodent models of PD [2], whereas in the focal dystonia benign essential blepharospasm, motor adaptation is enhanced [3]. Therefore, understanding the neural mechanisms behind motor adaptation in a motor behavior shared by all mammals that exhibits the same deficits in animal models as in PD patients may provide insight into treatment options. Blinking is an evolutionarily conserved behavior. It evolved to ensure corneal moisture in the face of evaporation when vertebrates moved out of the water onto the land. The same pattern of blinking is present in vertebrates as diverse as frogs and humans [4]. Thus, the trigeminal blink reflex provides an ideal model to study the neural bases of motor adaptation in normal and pathological states.

Forces Controlling Eyelid Movements

There are four forces that interact to produce the blinks that spread the tear film. Three active forces are produce by three muscles; the orbicularis oculi muscle (OO), the levator palpebrae superioris (LP) and Mueller's smooth muscle. OO contraction closes the eyelids. OO motor units are almost exclusively fast phasic. The motoneurons innervating the OO are found in the ipsilateral, dorsolateral facial motor nucleus. Contraction of the LP raises the upper eyelid. Motoneurons innervating the LP are in the oculomotor nucleus. Unlike the skeletal OO muscle fibers, LP muscle fibers are typical extraocular muscle

fibers [5, 6]. Mueller's muscle bridges the LP and the tarsal plate. Contraction of this muscle elevates the upper eyelid. Innervation of Mueller's muscle arises from the superior cervical ganglion [7]. Because the sympathetically controlled Mueller's muscle doesn't play a significant role in normal blinking [8], it will not be further discussed. The fourth force is a passive downward force. Opening the eyelids stretches several tendons and check ligaments to create a passive downward force, similar to pulling a bow string. To close the eyelid with a blink, the tonically active LP relaxes and the OO contracts. LP relaxation releases the passive downward forces. The combination of passive downward forces and the burst of OO activity lead to rapid eyelid lowering. To open the eyelid, the OO relaxes and LP motoneurons resume their tonic discharge (*Figure 1*). The contraction of the LP raises the eyelid. A balance between the LP tonic upward force and opposing passive downward forces created by lid elevation determines final upper eyelid position [8] [9]. Thus, the OO, LP, and passive downward forces work together to create eyelid movements with blinking and vertical eye movements. The similar anatomical organization of the eyelids among mammals suggests that neural circuits controlling the eyelids are also shared among mammals[8] [4].

Different Types of Blink

Based on when they occur and their kinematic properties, there are three types of blinks, voluntary, reflex and spontaneous. Voluntary blinking is the result of a conscious decision to blink. Reflex blinking is initiated by trigeminal, auditory, or visual stimuli. Spontaneous blinking occurs in the absence of external stimuli or conscious decision. In normal humans, the average spontaneous blink rate is approximately 14 blinks per minute and 5.3 blinks per minute in normal rats [10] [11]. Unlike voluntary and reflex blinks, spontaneous blinks appear to result from the activity of an endogenous blink generator, similar to central pattern generators [12] [11, 13, 14] that is modulated by corneal afferents, dopamine and cognitive states [11] [10, 15-18].

Blink Kinematic Differences in Voluntary, Spontaneous and Reflex Blinks

Although eyelid motion with blinking is similar for all types of blinks, there are kinematic differences among voluntary, spontaneous and reflex blinks [8]. There is a linear relationship between blink amplitude and maximum velocity for all three blink types. The peak velocity of lid closing increases with blink amplitude, but the slope of this relationship differs among the three types of blinks [8]. At the same blink amplitude, the peak velocity of reflex blink closing is fastest, followed by voluntary and finally by spontaneous blink lid closure [8]. Unlike the peak velocity of lid closure, however, the duration of the downward lid movement does not increase with blink amplitude. Nevertheless, there is a difference in downward lid movement duration among the three blink types. The lid lowering phase of spontaneous blinks has a longer duration than the other two types of blink [8].

Lid opening also shows a relationship between blink amplitude and peak velocity for the three types of blinks. Unlike with lid closure, however, there is no significant difference between the slopes for the three blink types. It requires less time to complete a downward lid movement of a blink than to accomplish an equal amplitude upward lid movement [8]. The downward lid movement is faster than the upward lid movement because there are two forces acting to close the eyelid [8, 9]. The OO muscle provides an active downward force and LP relaxation enables the passive downward forces to assist lid closure. In contrast, the LP must work against the passive downward forces with upward lid movement.

The pattern of orbicularis oculi electromyographic (OOemg) activity determines the kinematics of lid closing. The peak OOemg amplitude correlates with peak lid closing velocity. The OOemg activity for reflex blinks has an abrupt onset and achieves a large peak amplitude [8]. In contrast, the OOemg for voluntary and spontaneous blinks displays a slower buildup of activity and does not achieve as large a peak OOemg amplitude as reflex blinks [8]. The duration of lid closure corresponds to the duration of OOemg activity [8]. The integral of OOemg activity correlates with lid closing amplitude and peak closing velocity correlates with peak OOemg activity [8]. Whether a blink is voluntary, reflex or spontaneous, all blinks

have a similar pattern and investigators use different types of blinks to investigate brain circuits. This thesis focuses on trigeminal reflex blinks.

Orbicularis Oculi R1 and R2 Component in Primates and Non-Primates

In humans and rodents, stimulation of the supraorbital (SO) branch of the trigeminal nerve, elicits two OOemg responses, an initial component, R1, followed by a second component, R2 (*Figure 2*) [19-21]. In primates, the R1 response is usually small and the R2 response is large [8, 21-23]. In non-primate mammals, however, the R1 response is larger than the R2 [19] [24] [20, 25, 26]. In primates, the R2 response causes most of the lid closure with a blink [22] [8], whereas in non-primates, the R1 response produces most of the lid closure [19]. Primate studies show that SO stimulation usually evokes an R1 only ipsilateral to the site of stimulation, whereas the R2 response occurs bilaterally [8] [21]. Nevertheless, the R1 can be observed on the contralateral side if the OO motoneurons are depolarized [27] [28]. This observation indicates that the R1 response in primates is bilateral, but the contralateral R1 has a much higher threshold than the ipsilateral R1 [23, 29] Although special procedures such as bilateral eyelid closure are typically necessary to see the contralateral R1 in primates [27, 28], increasing the threshold stimulus intensity necessary to evoke an ipsilateral R1 by a factor of three elicits a contralateral R1 in non primate mammals[19, 20]. These data demonstrate that the contralateral R1 response is weaker than the ipsilateral and reinforce the proposal that trigeminal reflex blinks possess similar neural underpinnings in both primates and rodents [4] [20].

Three Subdivisions of the Trigeminal Nerve

The trigeminal nerve consists of three subdivisions: ophthalmic, maxillary and mandibular. The subdivisions of the trigeminal nerve convey nociceptive, temperature and touch modalities from the skin of

the face, the eyes, the dura, and the nasal cavity [30]. The ophthalmic branch of the trigeminal nerve carries sensory information from the skin of the upper eyelid, cornea, conjunctiva and the nose. The ophthalmic nerve also supplies sensory information from portions of the dura [30]. The maxillary nerve innervates the upper lip and upper jaw and the mandibular nerve innervates the lower part of the mouth [30]. One nerve in the ophthalmic branch of the trigeminal nerve is the frontal nerve that gives rise to the SO. The SO relays information from the forehead, upper eyelid and scalp (*Fig 3*). The primary afferents of the SO branch terminate in the brainstem in the spinal trigeminal nucleus, the dorsal horn of spinal cord C1 and the reticular formation [19, 31-35]. The spinal trigeminal nucleus complex is comprised of the principal and spinal trigeminal nuclei. The spinal trigeminal nucleus consists of three subnuclei, oralis, interpolaris and caudalis that extend caudally from the principalis to the dorsal horn of C1 [19, 30, 36]. Most trigeminal afferents split in the trigeminal tract and send processes to both the principalis and spinal trigeminal nuclei, however, some only project caudally and do not project to the principalis [37]. The SO nerve exhibits a bipartite termination pattern, innervating neurons in the border region between the interpolaris and caudalis subdivision and in the border region between caudalis subdivision of the spinal trigeminal nucleus and C1 spinal cord [34] [35] [32] [33] [20] [31] [19].The SO along with other ophthalmic branch afferents form the sensory limb of the trigeminal blink reflex [19].

The efferent limb of the trigeminal blink reflex eye closure, OO motoneurons, lie primarily in dorsolateral subdivision of the ipsilateral facial (VII) motor nucleus [38] [39, 40] [31, 41, 42]. During the R1 and R2 components of a SO evoked blink, individual OO motor neurons are active with both the R1 and R2 reflex blink components [38, 43] [44]. Even though individual OO motoneurons discharge with both the R1 and R2 blink components, the R1 and R2 responses arise from distinct neural circuits [45, 46] [19, 47]

Neurons in the border region between the caudalis/ interpolaris subdivision of the spinal trigeminal nucleus give rise to the R1 response, whereas the R2 response originates from neurons in the caudalis / C1 border region. Pellegrini et al. (1995) showed that hemisections of the caudalis / C1 region eliminated the

R2 but not the R1 response, whereas hemisections at the caudalis / interpolaris border region eliminated R1 as well as the R2 responses. To determine whether silencing the SO afferents at the interpolaris/caudalis could eliminate R1 only, Pellegrini et al. (1995) microinjected baclofen at the site of the SO interpolaris / caudalis termination zone. This injection initially reduced the R1, but not the R2 response [19]. This reduction in R1 amplitude presumably occurred because the $GABA_B$ agonist inhibited neurotransmitter release from SO pre-synaptic terminals in the interpolaris / caudalis border region.

The efferent connections of neurons in the trigeminal complex are the critical link between the afferent and motor elements of the trigeminal blink reflex [19]. There are direct projections to the OO motoneurons from the ipsilateral trigeminal nuclei [48] [49] [19] [50] [51]. Physiological experiments indicate that these neurons may be responsible for initiating the R1 of SO evoked blinks [19] and the initial component of corneal blinks [52] [51]. Neurons in the spinal trigeminal nucleus activated by the SO nerve also send projections to the reticular formation [19] [53]. The reticular neurons project to OO motoneurons and are responsible for the R2 [19] [53]. The spinal trigeminal nucleus also sends outputs to other brain regions that modulate trigeminal reflex blinks.

Spinal Trigeminal Nucleus Projections

Other outputs from the spinal trigeminal nucleus include projections to the contralateral inferior olive[54] [55] [56] [57], ipsilateral cerebellum [54, 56-58] [59] [60] and predominantly the contralateral superior colliculus [57, 61]. These brain regions modify the trigeminal blink reflex circuit.

The mammalian inferior olive (IO) is made up of the principal olive, the dorsal and the medial olive. Each olivary subnucleus projects contralaterally to one or more regions in the cerebellar cortex [62] [63] [64] [65]. Neurons in the oralis subdivision of the spinal trigeminal nucleus project to the border between the dorsal and principal IO, whereas neurons in the interpolaris subdivision project to the rostral-medial region of the dorsal olive, and neurons in the caudalis subdivision project to the medial part of

principal olive [54-56]. These data demonstrate that different regions of the trigeminal nucleus innervate different parts of the contralateral inferior olive.

Somatosensory information from the face reaches the Purkinje cells in cerebellum through mossy and climbing fibers. Trigeminal information goes to the cerebellum via mossy fibers from different subdivisons within the trigeminal nucleus [54, 57] [56, 66] [67] and the climbing fibers from the inferior olive that receive trigeminal inputs [66] [56] [54] [55] [57]. Trigeminal information conveyed through both mossy and climbing fibers are critical for the cerebellum's role in modulating the trigeminal reflex blink circuit.

Cerebellar interpositus neurons [68] [69] [70] send an excitatory projection to the contralateral red nucleus, which sends an excitatory input to OO motoneurons on the same side of the brain as the IP neurons [71, 72]. The cerebellum modulates blinking by altering the depolarization of the ipsilateral lid closing orbicularis oculi (OO) motor neurons in the facial nucleus via the red nucleus. The contralateral red nucleus also projects to the ipsilateral spinal trigeminal nucleus where it appears to cause inhibition [73](*Figure 4*).

The Red Nucleus (RN) receives a major input from cerebellar deep nuclei and links the cerebellum to OO motoneurons and the trigeminal complex. The RN is divided into two subnuclei, the parvocellular RN (pRN) located in the diencephalon and the magnocellular RN (mRN) in the mesencephalon. There are GABAergic and glutamatergic neurons in the pRN. The mRN contains only glutamatergic neurons [72] [74]. The neurons in the RN receive inputs from the sensorimotor cortex and the cerebellum and send afferents to spinal cord interneurons and motor neurons through the rubrospinal tract [75] [76-79] [80] [81]. RN anatomical studies demonstrate that rubrospinal tract fibers terminate in the dorsal horn (laminae V-VI), [75, 76, 82-86] spinal trigeminal nucleus [84, 87-89] and the facial nucleus [49, 85, 90]. The RN exhibits a somatotopic organization, the dorsomedial RN projects to cervical cord and the ventrolateral RN projects to lumbosacral spinal segments [91-95]. The RN terminal distribution suggests that rubrospinal neurons may modulate the responses of dorsal horn and spinal trigeminal neurons involved in the relay of

information to rostral levels of the nervous system. RN microstimulation inhibits neurons in the oralis subdivision of the trigeminal subnucleus [73] and neurons in the dorsal horn [96] . These data show that the RN inhibitory input to the trigeminal nucleus could influence the trigeminal blink reflex.

In addition to cerebellar and RN modulation of trigeminal reflex blinks, the superior colliculus also modifies reflex blinking. The superior colliculus (SC) is a layered structure in the mammalian brain serving sensorimotor integration. The superficial layers (1-3) are related to visual functions [97] [98]. Deeper layers of the superior colliculus receive inputs from the spinal cord, brainstem and cortical areas.

Blink Plasticity (Excitability)

Studies show that spinal trigeminal neurons primarily project to the deeper layers of the lateral SC [61] [57]. The SC appears to use this trigeminal information to modulate the excitability of trigeminal reflex blinks. The paired stimulus paradigm is a form of blink reflex modulation that estimates trigeminal reflex blink excitability. Presenting two identical SO stimuli with a short interstimulus interval normally evokes a response to the second stimulus (test) that is smaller than the response to the first stimulus (condition) (*Figure 5*) [2, 99, 100] [101] [20]. The second response is smaller because trigeminal blink circuits transiently reduce their trigeminal sensitivity following a blink. The fact that every blink creates trigeminal stimuli that could initiate a reflex blink necessitates this momentary reduction. Briefly reducing trigeminal sensitivity after each blink will prevent spasms of trigeminal reflex blinks. There is a three neuron circuit involving the SC [102] [103] [104] that can modulate trigeminal reflex blink excitability. With each reflex blink, neurons in the trigeminal complex send an excitatory input to SC neurons. The activated SC neurons excite neurons in the Nucleus Raphe Magnus (NRM) that increase inhibition of spinal trigeminal blink circuits through a serotonergic input [104]. In response to a pair of SO stimuli with a short interstimulus interval, this circuit ensures that the second SO stimulus will be less effective than the first because of NRM inhibition. In PD patients [100, 105] [106] and rodent models of PD (*Figure 5)* [20] [2], the trigeminal

reflex blink circuit becomes hyperexcitable. When presenting pairs of identical stimuli to the SO nerve, the response to the second stimulus is as large as or larger than the response to the first stimulus in PD patients. The basal ganglia affect trigeminal reflex blink excitability through an inhibitory input to the SC from the substantia nigra pars reticulata (SNr). The loss of dopamine in PD increases SNr activity and this increased inhibitory output decreases the activity of SC neurons in response to trigeminal input. The loss of SC excitatory drive on NRM neurons removes some of the inhibition to spinal trigeminal nucleus, leading to reflex blink hyperexcitability [102] [20, 104].

Blink Plasticity (High Frequency Stimulation)

The gain of the trigeminal reflex blink circuit can undergo long lasting changes by an appropriately timed train of stimuli to the SO nerve. Mao and Evinger (2001) presented high frequency stimulation (HFS) of the SO relative to the R2 component to produce associative modification in trigeminal reflex blinks in humans. Depending on the timing of when HFS was presented relative to R2 response, HFS could depress, potentiate or have no effect on the trigeminal blink reflex. Mao and Evinger (2001) showed that a series of 400 Hz SO stimuli occurring immediately before the R2 response (HFS-B) reduced the amplitude of subsequent SO-evoked blinks. Delivering HFS during the R2 (HFS-D) potentiated subsequent blinks SO-evoked blinks and applying the HFS after the R2 (HFS-A) didn't alter the response of subsequent SO-evoked blinks (*Figure 6*). HFS of the SO modified trigeminal reflex blink amplitude for at least one hour [107]. These changes developed unilaterally in the trigeminal blink circuits. For example, when HFS was delivered to the left SO, a subsequent blink-evoking stimulus to the left SO elicited modified blinks in both eyelids. Stimulation of the right SO that did not receive HFS, however, evoked normal blinks in both eyelids. These HFS induced modifications in trigeminal reflex blink amplitude were gain changes because the blink evoking stimulus was the same before and after the HFS paradigm while blink amplitude underwent modification.

HFS training modified trigeminal reflex blink gain in rats the same way as occurred in humans. Ryan et al., (2014) investigated the effects of HFS-B on the R1 response of the blink reflex. The rats that underwent HFS-B treatment exhibited decreased R1 amplitude relative to pre-HFS R1 values in the first hour after training, (*Figure 7*). As with humans, HFS-A did not affect subsequent blink amplitude [108] [107].

Gain Modification Involving the Cerebellum

Ryan et al (2014) investigated whether the cerebellum participated in reflex blink gain modifications during HFS-B training. The cerebellum is critical in delay eyelid conditioning in which a subject learns that an innocuous conditioned stimulus predicts the occurrence of a blink evoking unconditioned stimulus [109] [110-112]. Ryan et al (2014) tested whether using HFS-B as the unconditioned stimulus in delay eyelid conditioning affected eyelid conditioning, HFS-induced blink depression, or both. If eyelid conditioning that increases blink amplitude and HFS-B training that depresses blink amplitude share neural circuits, then there should be occlusion of both types of learning. Eight rats underwent delay eyelid conditioning in which the HFS-B stimulus co-terminated with a tone. The tone served as the conditioned stimulus and the HFS-B served as the unconditioned stimulus. The rats were divided based on whether they achieved more than 70% CRs in twelve days of training, conditioning. The rats that did not achieve 70% CRs over 12 days of training did not show conditioning. These rats showed overall depression in blink amplitude; however, this blink depression was significantly less than the blink depression created by HFS-B training alone. In contrast, rats that achieved over 70% CRs showed an insignificant reduction in blink amplitude with HFS, but developed eyelid conditioning much more slowly than rats in a typical eyelid conditioning paradigm. Despite both groups receiving HFS-B stimulation, there was a smaller than normal reduction in blink gain with poorly conditioned rats and no change in blink gain

with better-conditioned rats [108]. This result indicated that HFS gain adaptation and delay eyelid conditioning shared similar circuits, most likely in the cerebellum.

There is abundant evidence that the cerebellum is critical for delay eyelid conditioning and is also essential for gain changes of the trigeminal blink reflex and other motor systems. Cerebellar interpositus nucleus lesions prevent delay eyelid conditioning and block expression of previously acquired eyelid conditioning [109] [110] [111, 112]. IP neuron discharge patterns are appropriate to support delay eyelid conditioning and gain changes of blink reflexes [113, 114]. An example of the role of the cerebellum in gain changes in other systems is that a lesion of the vestibulocerebellum prevents gain adaptation of the vestibuo-ocular reflex [115, 116]. Similarly, damage to the vermis or fastigial nucleus disrupts saccadic gain adaptation [117] [118] and neurons in these regions modify their discharge properties appropriately to account for these gain changes. Finally, lesions of the cerebellar cortex prevent trigeminal reflex blink gain increases [119]. Thus, the cerebellum is critical in gain modification.

Cerebellar Interpositus Nucleus in Blink Modulation

The IP works with the trigeminal blink circuit to regulate blink gain. The cerebellum modulates blinking by its effect on the lid closing OO motor neurons in the facial nucleus. IP neurons send an excitatory projection to the contralateral RN that sends an excitatory input to OO motoneurons on the same side of the brain as the IP neurons[71, 72]. Spinal trigeminal sensory information is conveyed to the cerebellar cortex and the interpositus nucleus via mossy fibers and climbing fibers from the inferior olive [54] [55] [56, 57]. A specific group of IP neurons, named Pause neurons, are tonically active neurons that transiently cease firing slightly before the end of trigeminal reflex blink OOemg activity. The tonic activity of the IP neurons sets a baseline for OO motoneuron depolarization to increase or decrease blink amplitude and the transient pause in activity helps regulate blink duration. In anesthetized rats, restraint of the eyelid leads to an increase in blink reflex gain. In this paradigm, pause neurons exhibit an increase in tonic activity

and a delay in the transient pause preceding blink termination [113]. This pattern of activity supports the increased amplitude and longer duration reflex blinks necessary to increase blink gain. These changes in IP activity appear to be responsible for the increased reflex blink gain and may be responsible for the gain changes induced by HFS-B training.

c-Fos Neuronal Activation

Based on previous research on the HFS-B paradigm and the cerebellar modulation of the trigeminal blink circuit, I wanted to identify neurons activated in the HFS-B modification of the trigeminal circuit. I utilized c-Fos immunohistochemistry to assess neuronal activation of the spinal trigeminal nucleus, inferior olive and the red nucleus. c-Fos is cellular proto-oncogene belonging to the immediate early gene family of transcription factors [120] [121]. Using immunohistochemical techniques, the protein can be detected in a neuron's nucleus following neuronal activation [121] [120] [122] [123] [124]. c-Fos protein is rapidly, but transiently induced in both excitatory and inhibitory neurons in response to a variety of noxious and non-noxious stimuli, growth factors and second messenger signaling [124] [125, 126] [127] [128] [129]. *In vitro* experiments indicate that c-Fos activation is rapid and transient. In cell culture, gene expression starts within a few minutes of cell stimulation and returns to baseline within two hours even with persistent stimulation. Other investigators suggest that the pattern of c-Fos expression in the intact animal might be slower than in *in vitro* [130] [131] [132] [133]. Noxious stimuli induce c-FOS like immunoreactivity that appears rapidly following the onset of the stimulus and remains 16-24 hours [125] [124]. Using a high intensity electrical stimulation with stimulus durations ranging from 3 seconds to 24 hours to activate nociceptors without damaging the spinal cord in rats shows that stimulus duration has a profound effect upon cell activation [134]. For example, a short stimulus lasting 3 seconds induces a small number of c-Fos cells, whereas a longer stimulus at the same current lasting for 20 minutes induces more cells than the 3 second stimulus. A stimulus duration of 4.5 hours produces the maximum c-Fos induction and stimulus

durations ranging from 6.5 to 24 hours produces fewer cells than the 4.5 hr stimulus. These results indicate that c-Fos activation may be affected by the duration of the exciting stimulus [134]. Another study shows that c-Fos expression is higher in rats receiving a noxious stimulus compared to those receiving a non-noxious stimulus. Rats in this study underwent severe spinal contusion at the 8^{th} thoracic spinal level. c-Fos activation was observed below the injury site in response to either noxious electrical, chemical (formalin) or non-noxious stimulation (brushing). The dorsal horn cells below injury site that received noxious stimulus (electrical or chemical) had more c-Fos labeled cells compared to the non- noxious stimulus [135]. Another study demonstrated electrical stimulation of the SO nerve in rats followed by c-Fos immunohistochemistry was used to identify the distribution of activated neurons in the spinal trigeminal nucleus and C1 cervical spinal cord. In this study rats that received stimulation of SO nerve exhibited a higher number of neurons expressing c-Fos in the ipsilateral spinal trigeminal nucleus. The SO stimulated rats also exhibited bilateral c-Fos activation in the caudalis region of the spinal trigeminal nucleus [136]. In summary c-Fos expression is an indicator of neuronal activity for both innocuous and noxious stimuli.

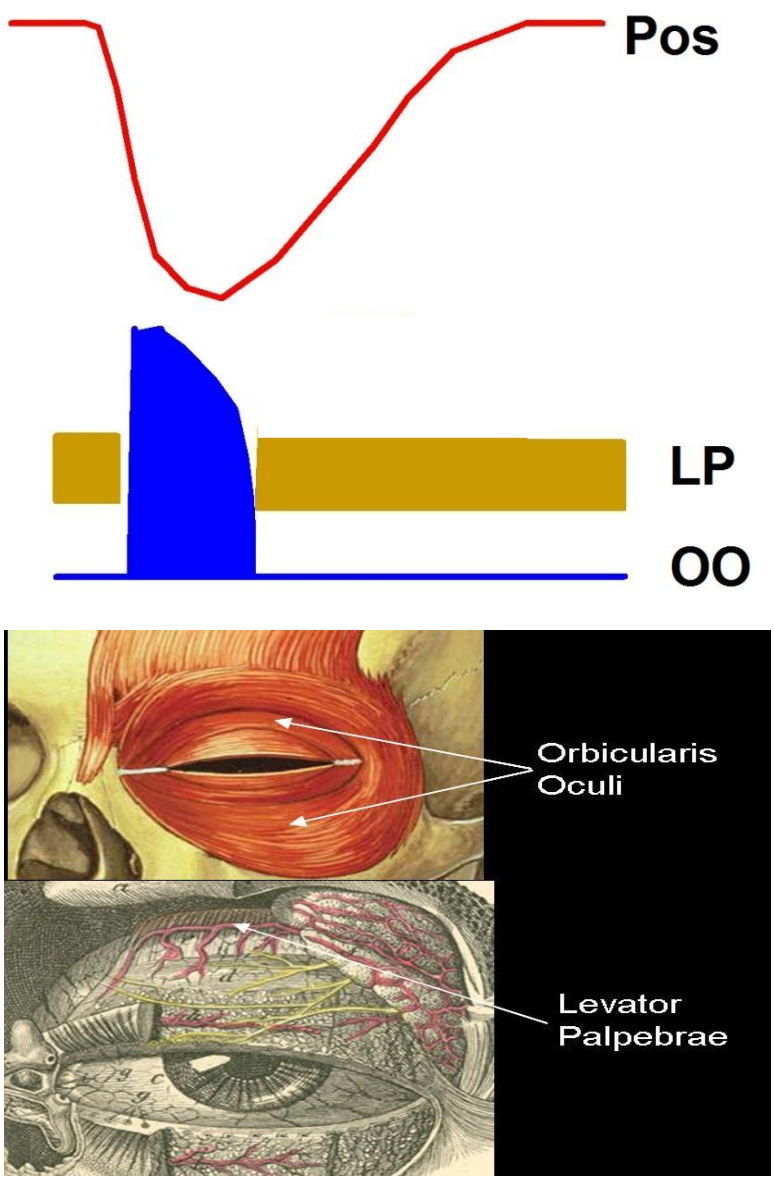

Fig. 1. Mammalian blinking (Evinger et al., 2010) [137]. Upper eyelid position (Pos) lowering during a blink results from a transient relaxation of the Levator Palpebrae (LP) followed by a phasic activation of the Orbicularis Oculi (OO) muscle. Raising the eyelid occurs as the LP resumes its tonic activity following the completion of the OO activity. Gold indicates LP activity and blue OO activity. (Bottom) A drawing showing the OO (upper) and LP (lower) muscles.

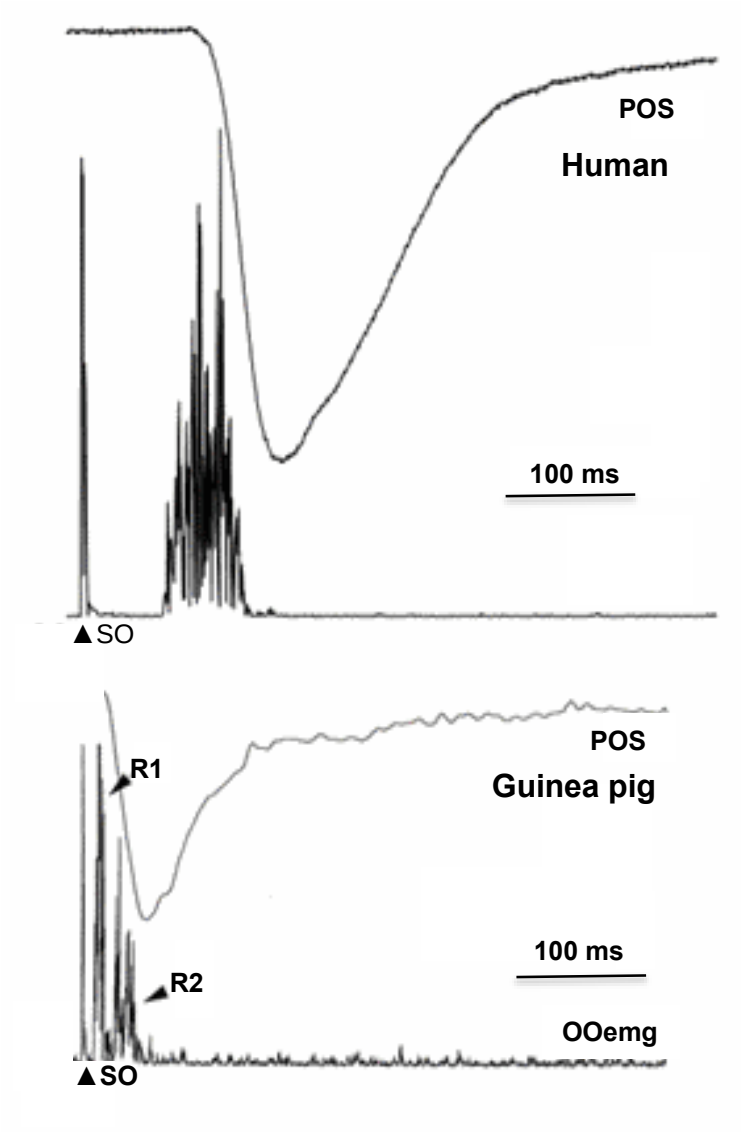

Fig. 2. (Evinger et al., 2010) [137]Examples of a reflex blink evoked by stimulation of the supraorbital branch of the trigeminal nerve (▲SO) for a human and a guinea pig. OOemg, orbicularis oculi electromyographic activity; Pos, upper lid position; R1, 1st OOemg response; R2, 2nd OOemg response; SO, supraorbital nerve stimulus

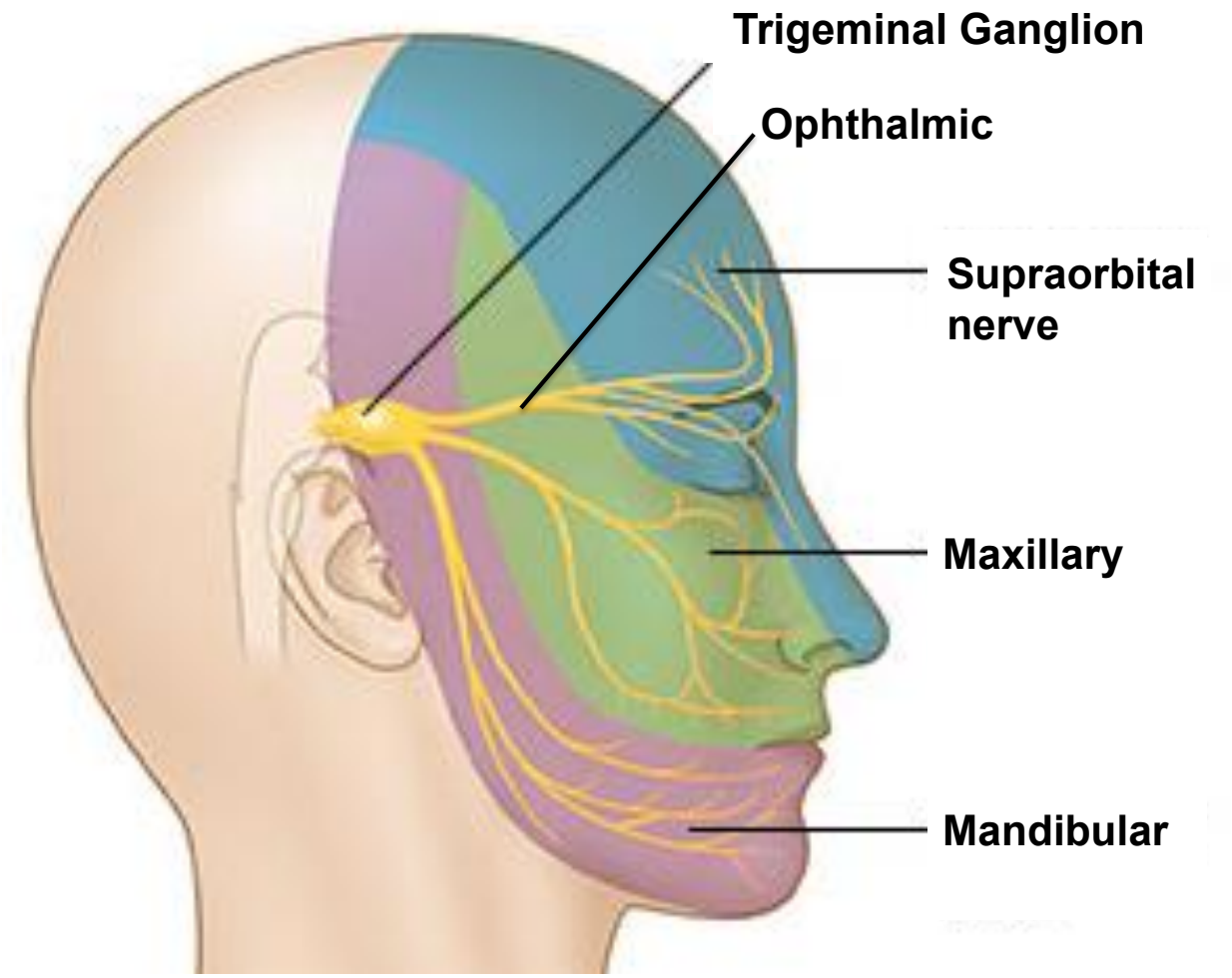

Fig. 3. Adapted from Trigeminal Neuralgia [138] Three divisions of the trigeminal nerve, Ophthalmic, Maxillary and Mandibular branch innervating the face and forehead. The supraorbital nerve arises from the frontal nerve of the ophthalmic branch.

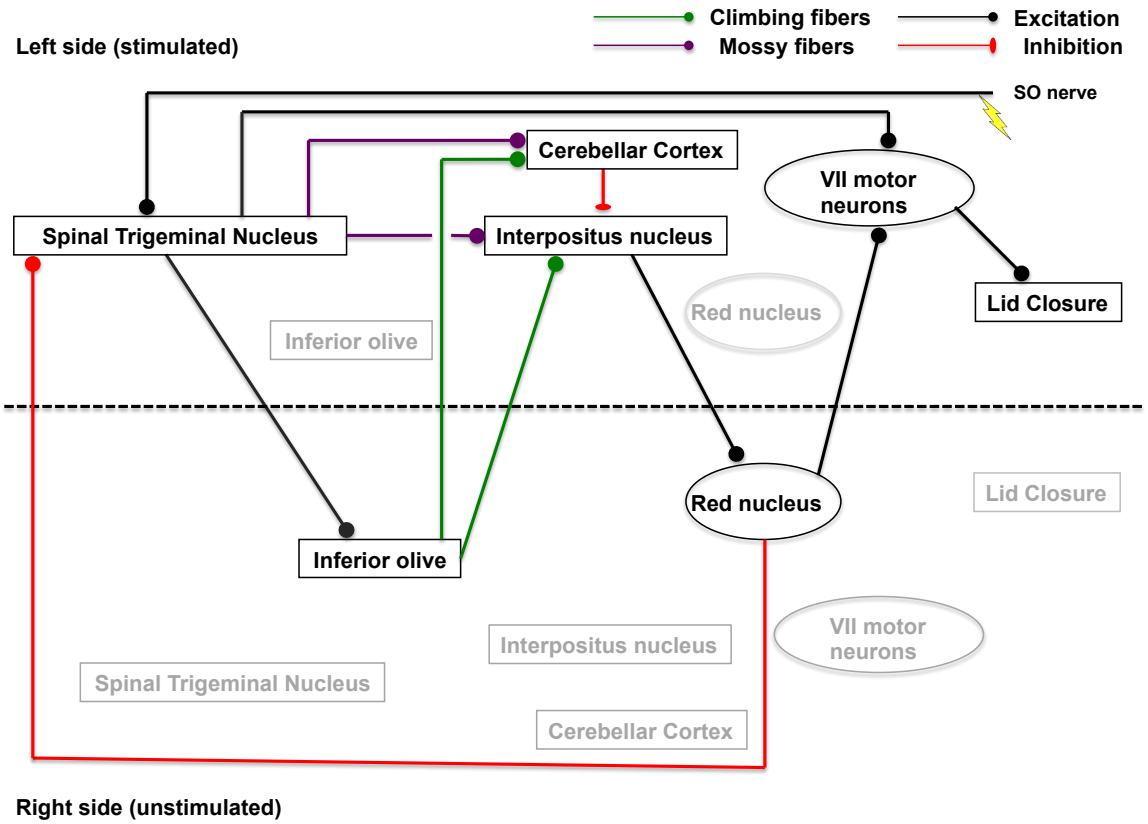

Fig. 4. Circuit diagram of the cerebellum and the spinal trigeminal nucleus connections involved in trigeminal reflex blinks.

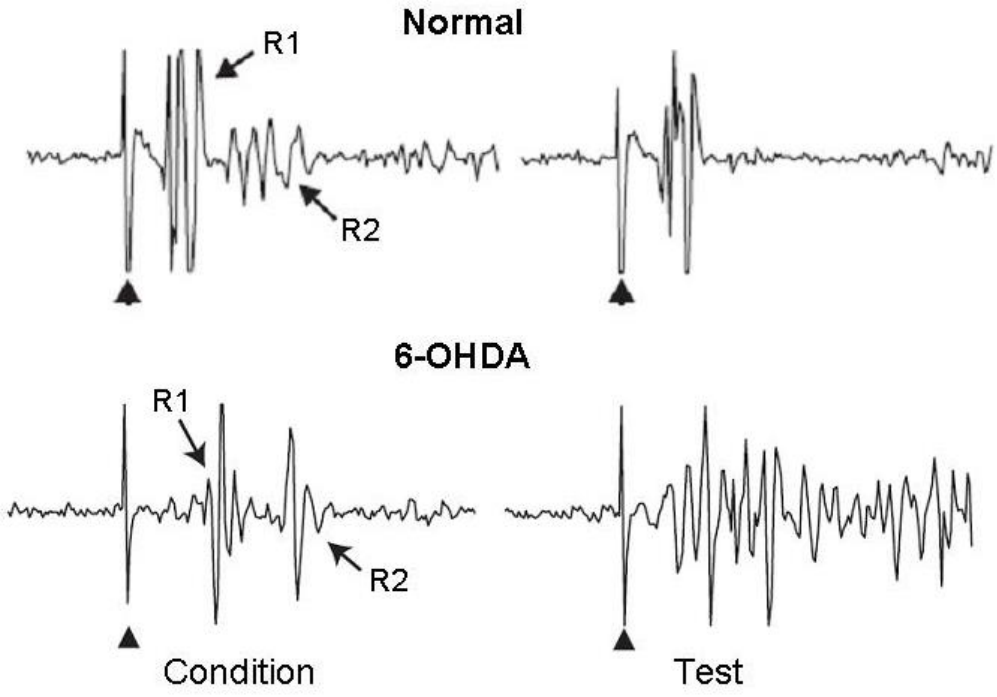

Fig. 5. Kaminer et al., 2015, Kaminer et al., 2014[139] [2]. Response to paired stimulation of the supraorbital branch (▲SO) of the trigeminal nerve in normal and 6-OHDA lesioned rats. The R2 response to the 2nd SO stimulus is larger than the response to the 1st SO stimulus in the 6-OHDA rat. EMG data are rectified and averaged. Abbreviations: 6-OHDA, 6-Hydroxydopamine; OOemg, orbicularis oculi electromyographic activity; R1, 1st OOemg response; R2, 2nd OOemg response; SO, supraorbital nerve stimulus;

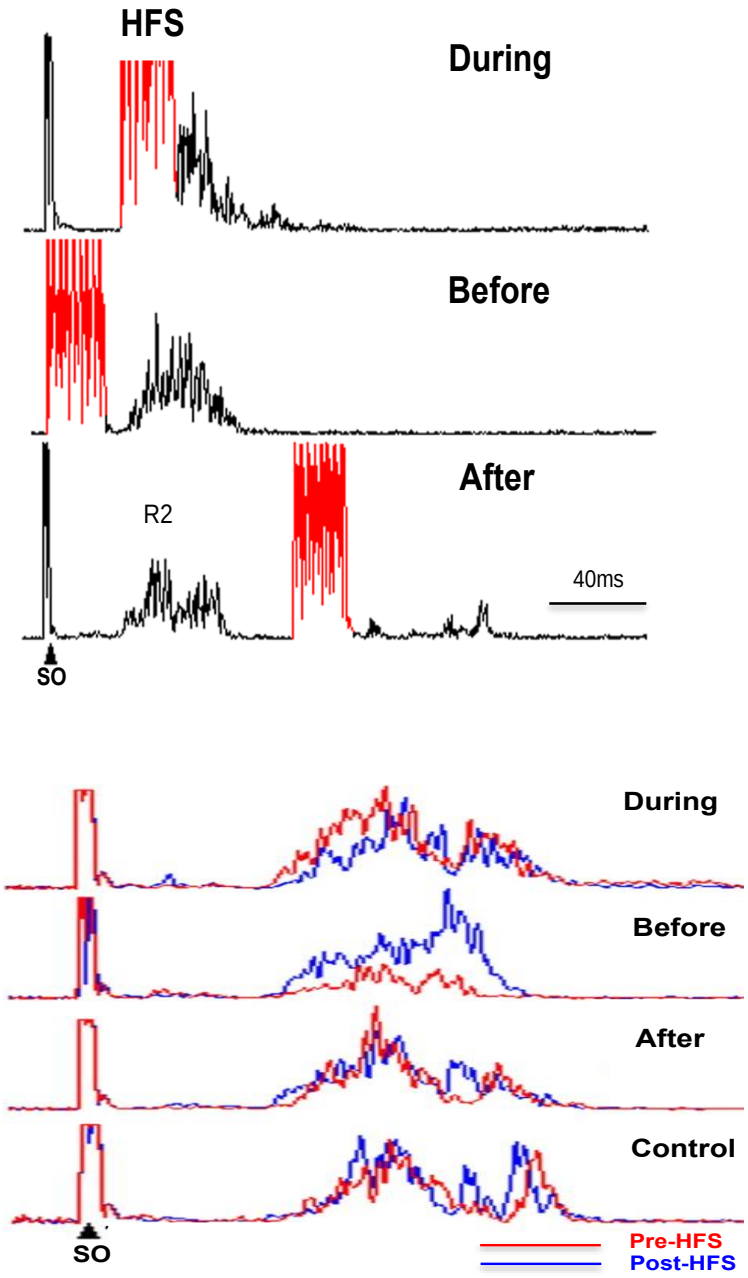

Fig. 6. Evinger and Mao, 2001 [107] (Upper) High frequency stimulation of the supraorbital nerve (HFS) treatment relative to R2 component in humans, HFS-D (During), HFS-B (Before) and HFS-A (After). (Bottom) Stimulated supraorbital nerve (SO) after different HFS treatments. Abbreviations: HFS, High Frequency Stimulation OOemg, orbicularis oculi electromyographic activity; R2, 2nd OOemg response.

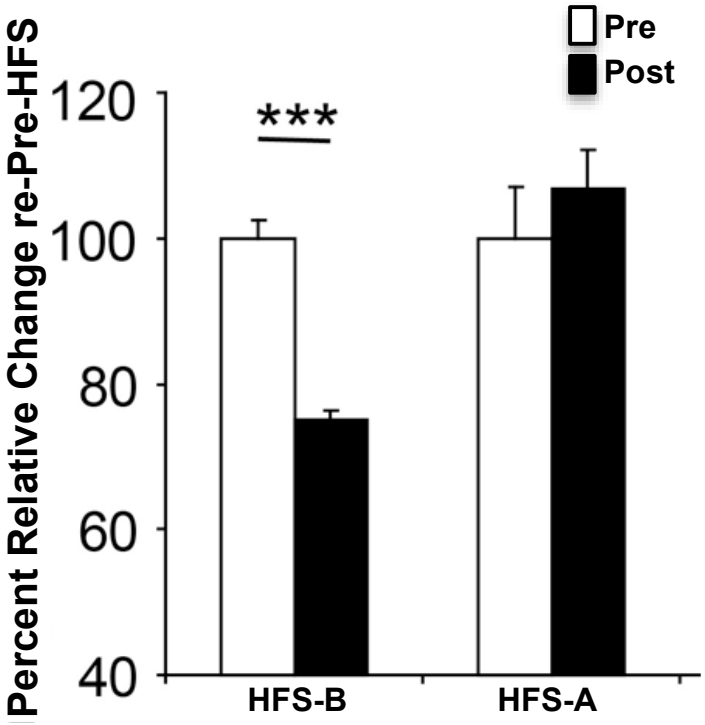

Fig. 7 Ryan et al., 2014 [108] Average short term gain change in R1 blink amplitude following HFS training (Post) relative to average pre HFS R1 amplitude (Pre). *** $p < 0.001$. Error bars are SEM; Abbreviations: HFS-A, High Frequency Stimulation after R2; HFS-B, High Frequency Stimulation before R2

Materials and Methods

Experiments were performed on nine male Sprague Dawley rats (350-550g) maintained on a reversed 12-hour light/dark cycle and fed ad libitum. All experiments received approval by the Stony Brook University Institutional Animal Care and Use Committee and complied with all Federal, State and University regulations and guidelines regarding the use of animal in research.

Surgery

Under general anesthesia, ketamine 90mg/kg and xylazine 10mg/kg, rats were prepared for chronic recording of the left orbicularis oculi electromyogram (OOemg) and stimulation of the left supraorbital branch of the trigeminal nerve (SO) [139] [8, 20, 108]. The SO nerve was exposed and enclosed in a Teflon nerve cuff containing a pair of stainless steel wires. A pair of Teflon coated stainless steel wires was implanted into the left orbicularis oculi (OO) to record the OOemg. All the wires were led subcutaneously to a connector embedded in a dental acrylic platform on the skull. The platform was attached to the skull by four stainless steel screws and a silver wire was attached to one of the screws to serve as a ground. To relieve any postoperative discomfort, all rats received ketorolac (7mg/kg) twice daily for two days or longer if the rats continued to exhibit signs of discomfort. Depending on postoperative recovery of each rat, rats will begin behavioral testing two days after the surgery.

Behavioral Testing

Reflex blinks were monitored as rats moved freely in their home cage in a darkened room during their subjective night. OOemg signals were amplified 10,000 and filtered from 0.3-5 kHz. SO stimuli were 100μs in duration and current intensity was set at the start of each experimental day as the threshold (T) current necessary to evoke a R1 blink component reliably. All data were collected at twice the threshold current (2T). Rats then received 12 trials of a pair 2T SO stimuli with a 100 ms interstimulus interval. The intertrial interval for the 12 trials varied pseudorandomly over the range of 20 ± 5 ms. Rats underwent three days of testing with 12 trials of pairs of SO stimuli.

On the fourth day, rats were assigned to a paradigm developed for humans [107] and modified for rodents [108] to decrease blink gain (n=4; Fig. 8B) or a control condition (n=5, Fig. 8C). To decrease reflex blink gain, rats received a 2T SO stimulus to evoke a reflex blink followed by a 400 Hz 2T SO stimulus train that began with the R1 response and terminated before the R2 component of the blink (HFS-B). For the control condition, rats received a single 2T SO stimulus (No-HFS). Each rat received 5 blocks of trials: (1) 20 trials of a pair of 2T SO stimuli with a 100 ms ISI (Pre-HFS); (2) 60 trials of 2T HFS (HFS) or 60 trials of a single 2T SO stimulus (No-HFS) treatment; (3) 20 trials of a pair of 2T SO stimuli with a 100 ms ISI immediately after HFS/No-HFS (T0); (4) 20 trials of a pair of 2T SO stimuli with a 100 ms ISI 30 min after the end of HFS/No-HFS treatment; and (5) 20 trials of a pair of 2T SO stimuli with a 100 ms ISI 60 min after the termination of HFS/No-HFS trials (*Fig 8D*) All trials were delivered with a pseudorandom 20 ± 5 ms intertrial interval. Immediately after the T60 trials, the rat was deeply anesthetized with ketamine 90mg/kg and xylazine 10mg/kg and intracardially perfused with 6% dextran in phosphate buffered saline to remove blood followed by 4% paraformaldehyde to fix the brain. After the perfusion, the rat brain was kept in 4% paraformaldehyde in 0.1M phosphate buffer (PB) for 1 hour. The rat brain was then transferred into 30% sucrose solution.

c-Fos Immunohistochemistry

After blocking, the brains were frozen and cut into 40μm coronal sections using a freezing microtome. Every fourth section was stained for c-Fos. All tissue was reacted free floating in net wells and all reactions occurred at room temperature. The tissue was incubated in 3% normal rat serum and 5% normal goat serum in 0.3% triton-X in PB phosphate buffer (PBX) for 30 to 60 min. Following three 10 min washes in phosphate buffer (PB), the tissue was incubated in primary antibody (Santa Cruz antibody c-Fos Polyclonal Rabbit) at a dilution 1:1000 in PBX. After three 10 min washes in PB, the tissue was incubated in secondary antibody (Vector biotinylated anti Rabbit made in goat) at a dilution 1:200 in PBX. After 30 minutes of washing in PB, the tissue was reacted with diaminobenzidene (DAB, 55mg/100ml) in PB for five minutes. Hydrogen peroxide (H_2O_2) was added to the DAB solution to make a final concentration of 0.03% H_2O_2 and the tissue was reacted in this solution for 3-5 minutes. Following six 10 min washes in PB, the sections were then mounted on gelatin-coated slides, left to dry overnight, and then dehydrated, cleared in xylene and cover slipped.

Data Collection and Analysis

OOemg signals were collected at 4 kHz per channel (DT 2831; Data Translation, Marlboro, MA; 12-bit analog-to-digital resolution), and stored for later offline analysis on laboratory-developed software. The OOemg latency and duration were determined by marking the stimulus artifact produced by the SO stimulus and the start and end of the blink. Blink amplitude was determined by integrating the rectified OOemg activity of each blink component. To determine if HFS treatment induced a change in reflex blink gain, all R1 blink amplitudes were normalized to the median R1 blink amplitude collected in the pre HFS

data block. Because Ryan et al (2014) demonstrated that there was no difference in blink amplitude in the T0, T30, and T60 blocks, post HFS R1 amplitude was averaged over all three post treatment blocks and normalized to the median pre HFS blink amplitude. The normalized mean pre HFS was subtracted from the normalized mean post blink amplitude. The change in blink amplitude following HFS was a gain change because the blink-evoking stimulus did not change throughout the experiment[108] .

Blink excitability was quantified by dividing the blink amplitude evoked by the second SO (test) by the blink amplitude evoked by the first SO (condition) for every trial. For each rat, pre HFS excitability was the median of blink excitability for all pre HFS trials. Post HFS excitability was the median of blink excitability for all T0, T30, and T60 trials for that rat.

c-Fos cell counting

The outlines of the spinal trigeminal nucleus, inferior olive and red nucleus were drawn using a camera lucida at a magnification of 25X and the location of *c-Fos* labeled cells were marked on the drawings. Each region of interest was identified using Paxinos and Watson rat brain atlas [140]. The drawings were then scanned and cells were counted using Image J (https://imagej.nih.gov). Cell density was calculated by dividing the total number of cells by the total area for each region. The area of each region was estimated by weighing a cutout of the region of interest. The weights were converted to cm^2 by using ImageJ to determine the relationship between paper weight and scanned area.

Statistical tests of significance ($p < 0.05$) were performed with SPSS software using an independent-samples t test and ANOVA. Data are presented as the mean ± SEM.

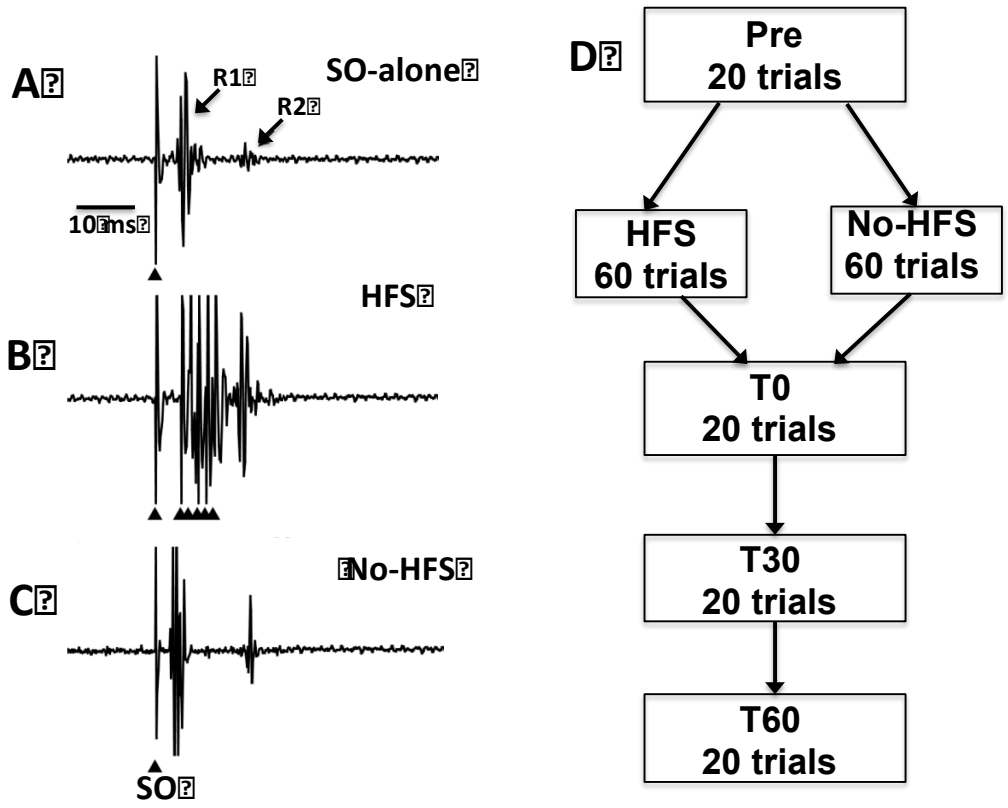

Fig 8. Treatment Paradigm (A) Supraorbital branch of trigeminal nerve (SO)-evoked blink with R1 and R2 components. (B) High Frequency Stimulation (HFS) presented before R2. (C) No-HFS. (D) Experimental paradigm. ▲SO, supraorbital nerve stimulus.

Results

The occurrence of c-Fos labeled neurons within the trigeminal nucleus was the initial focus of the research. To orient the reader to the location of the trigeminal complex and its subdivisions, Fig. 9 shows a horizontal section of the brainstem showing the trigeminal complex. Moving caudal to rostral, the regions of interest are C1 of the spinal cord, the caudalis subdivision, the interpolaris subdivision, the oralis subdivision of the spinal trigeminal nucleus and the principalis nucleus of the trigeminal. Because the primary terminations of the SO nerve in trigeminal occur caudal to the nucleus principalis [19, 31-35], cell counting focused on the region from -10 to -18 mm caudal to bregma.

c-Fos Neuronal Activation within Spinal Trigeminal Nucleus for HFS and No-HFS Rats

c-Fos labeled cell density was quantified along the length of the spinal trigeminal nucleus. Figure 10 shows the average density of c-Fos labeled cells in 640μm segments (3 sections) of the spinal trigeminal nucleus for the rats in the HFS group. For the trigeminal nucleus that received an input from the stimulated SO, (ipsilateral), c-Fos labeling appeared to differ along the length of the spinal trigeminal nucleus. Moving caudal to rostral, the highest density of labeled cells occurred at the posterior pole of the spinal trigeminal nucleus, approximately -17.3 mm caudal to bregma [140] . The minimum density of neurons occurred at -16 mm caudal to bregma, followed by a steady increase in the density of c-Fos labeled neurons moving forward to the rostral end of the spinal trigeminal nucleus, approximately -10 mm caudal to bregma (Fig. 10A). The pattern of c-Fos labeled neurons in the contralateral spinal trigeminal nucleus appeared similar except that the density of labeling decreased in the most rostral portion of the contralateral spinal trigeminal nucleus. This difference between the ipsilateral and contralateral sides for HFS rats, however, was not

statistically significant. The average density of labeled c-Fos cells across the entire spinal trigeminal nucleus was not significantly different between the spinal trigeminal nucleus receiving SO activation (ipsilateral) and the contralateral spinal trigeminal nucleus ($F_{(1)}$= .155, *p>0.05; Figure 10A*). The total average density in the ipsilateral spinal trigeminal nucleus was 182.4 ± 67.8 cells/mm^2 and the contralateral spinal trigeminal nucleus was 166.9 ± 70 cells/mm^2 ($T_{(6)}$= -.0.159, *p>0.05; Figure 10B*).

For the rats in the No-HFS condition (Figure 11), c-Fos labeling also appeared to differ along the length of the ipsilateral side of the spinal trigeminal nucleus. Moving caudal to rostral, the highest density of labeled cells occurred at the posterior pole of the spinal trigeminal nucleus, approximately -16.5 mm caudal to bregma [140]. The lowest density of neurons occurred at -14 mm caudal to bregma, followed by a steady increase in the density of c-Fos labeled neurons moving toward the rostral end of the spinal trigeminal nucleus, approximately -10 mm caudal to bregma (Fig. 11A). The contralateral spinal trigeminal nucleus appeared to have a similar pattern of c-Fos labeled neurons, except the density of c-Fos labeled cells decreased in the most rostral end of the contralateral trigeminal. In the HFS condition, the average density of labeled c-Fos cells across the entire spinal trigeminal nucleus was not significantly different between the ipsilateral and contralateral trigeminal for No-HFS rats ($F_{(1)}$= 2.094, *p>0.05; Figure 11A).* The total average density in the ipsilateral spinal trigeminal nucleus was 141.3 ± 26.9 cells/mm^2 and 136.9 ± 26.1cells/mm^2 in the contralateral spinal trigeminal nucleus ($T_{(8)}$= -0.117, *p>0.05; Figure 11B).* Given that the termination of the SO nerve is ipsilateral [34] [19, 33] [32] [31] [35], the c-Fos labeled neurons in the trigeminal contralateral to the SO stimulus for both the HFS and No HFS conditions appear to result from the interconnections between the spinal trigeminal nuclei [141].

To determine whether the HFS and No-HFS paradigms produced different patterns of c-Fos labeling within the stimulated spinal trigeminal nucleus, the ipsilateral HFS and No-HFS data were compared (Fig. 12). Going from caudal to rostral, the highest density of labeled cells occurred at the posterior pole of the spinal trigeminal nucleus in both the HFS and No-HFS conditions. Both HFS and No-HFS rats exhibited a steady increase in the density of c-Fos labeled neurons moving toward the rostral end

of the spinal trigeminal nucleus, approximately -10 mm caudal to bregma. In contrast, the lowest density of c-Fos labeled cells for the HFS rats occurred around -16mm, whereas the lowest density of No-HFS labeled neurons occurred at -14mm caudal to bregma. At all but two points in caudal spinal trigeminal nucleus, the average density of c-Fos labeled neurons was higher in the HFS condition than in the No-HFS condition. Nevertheless, the average density of labeled c-Fos cells across the entire spinal trigeminal nucleus was not significantly different between HFS and No-HFS conditions ($F_{(1)}$= 14.898, *p>0.05;Figure 12A*). The total average density within the entire spinal trigeminal nucleus ipsilateral to SO stimulation was 182.4 ± 67.8cells/mm^2 in the HFS condition and 141.3± 26.9 cells/mm^2 in the No-HFS condition ($T_{(7)}$= 0.615, *p>0.05;Figure 12B*).

Density of c-Fos Labeled Cells in Anterior and Posterior SO Termination Regions of HFS and No-HFS Rats

Because there were no significant differences between c-Fos cell density over the entire spinal trigeminal nucleus for the HFS and NO HFS groups, the regions of the trigeminal nucleus that received the densest terminations of SO primary afferents were examined. Gong and colleagues (2003) showed that the SO termination in the rat had two peaks within the spinal trigeminal nucleus [31]. The site of the largest area of SO termination in the anterior of spinal trigeminal nucleus occurred between -10.2 mm and -12 mm caudal to bregma, whereas the largest area of SO termination in the posterior region of the spinal trigeminal nucleus was between -13.3 and -15.5 caudal to bregma (Fig. 12A). The density of c-Fos labeled cells in anterior and posterior SO termination regions of HFS and No-HFS rats were compared to determine whether there were any differences in c-FOS cell density at the dominant sites of SO termination within the spinal trigeminal nucleus. For the stimulated spinal trigeminal nucleus, rats in the HFS condition exhibited a higher average cell density than did rats in the No-HFS condition in anterior termination zone (HFS: 189.7± 53.1 cells/mm^2; No-HFS: 140.2 ± 31.1 cells/mm^2). These differences, however, were not

statistically significant ($T_{(7)}$= -0.846, *p>0.05; Figure 13A*). In the posterior SO termination zone, rats in the HFS condition had an average cell density of 167.8± 79.3 cells/mm^2 compared to 110.3 ± 33.4 cells/mm^2 for the No-HFS condition. Nevertheless, this difference between HFS and No-HFS labeled cell density in the posterior termination region was not significant ($T_{(7)}$= 0.725, *p>0.05*). Within the HFS and No-HFS conditions, there were no significant differences between the c-Fos cell density in the anterior and posterior SO termination regions (HFS anterior vs. HFS posterior (ipsilateral), $T_{(6)}$= -0.229, *p>0.05*; No-HFS anterior vs. No-HFS posterior (ipsilateral), $T_{(8)}$= 0.655, *p>0.05;*Figure 13A)

Given the absence of a statistical difference between the average labeled cell density of the ipsilateral and contralateral trigeminal nuclei in the HFS and No-HFS conditions (Figs. 10B, 11B), it was not surprising that the contralateral spinal trigeminal nucleus also did not show significant differences in the c-Fos cell density between rats receiving HFS and No-HFS for the either the anterior or posterior regions of SO termination (Fig. 13B; HFS vs. No-HFS anterior, ($T_{(7)}$= 0.408, *p>0.05*; HFS vs. No-HFS posterior, $T_{(7)}$= 0.416 *p>0.05*). Within the HFS and No-HFS conditions, there was also no significant difference between average c-Fos cell density in the anterior and posterior segments of the spinal trigeminal nucleus (HFS anterior vs. HFS posterior (contralateral), $T_{(6)}$= -0.214, *p>0.05*; No-HFS anterior vs. HFS posterior (contralateral), $T_{(8)}$= -0.029, *p>0.05;*Figure 13B).

Gain Changes in HFS and No-HFS Rats

Based on the Ryan study [108], HFS-B modification of the trigeminal reflex blink created large gain decrease in the blink circuit. The goal of comparing cell activation in the HFS and No-HFS conditions was to create big differences in gain modifications between the two conditions. The density of c-Fos labeling in the spinal trigeminal nucleus as a function of the magnitude of gain change was determined independent of the HFS and No-HFS conditions. Three rats that received HFS-B treatment showed the expected decrease in gain of approximately -0.35 [108], but the 4th rat exhibited a 0.33 increase in gain

(Fig.14, ●). Because of this rat, the average gain for the rats in the HFS condition was -0.18 ± 0.20. In the rats that received the No-HFS treatment, four rats showed a smaller decrease in gain than did the HFS rats, approximately-0.13, but one rat exhibited a decreased gain like that of HFS treated rats, -0.43 (Fig.14, ■). Because of this last rat, the mean gain change for the No-HFS rats was –0.19 ± 0.06. Because of an extreme value in both of the two conditions, there was no significant difference in the gain change between the HFS and No-HFS conditions ($T_{(7)}$= 0.64, p<0.05*;Figure 15).* To test the hypothesis that the average density of c-Fos labeled cells correlated with gain change rather than treatment condition, rats were regrouped into gain decreases more than -0.2 (<-0.2) and smaller gain decreases (>-0.2.). This reorganization created two significantly different groups, rats with an average gain change of -0.37 ± 0.06 (n=4, <-0.2) and rats with an average gain change of -0.04 ± 0.1 (n=5, >-0.2) ($T_{(7)}$= -2.835, *p<0.05; Figure 15*).

c-Fos Cell Density as a Function of Gain Change in the Spinal Trigeminal Nucleus

Plotting average c-Fos cell density as a function of average gain change for the entire spinal trigeminal nucleus (Fig. 16A, ▲), the anterior SO termination zone (Fig. 16B, ●), and the posterior SO termination zone (Fig. 16B, ◆) revealed that increases in the density of c-Fos labeling correlated with greater gain change. For all three measurements, the rat with a gain increase (0.33) showed the lowest c-Fos labeled cell density, and the average density of c-Fos cells increased as gain decreases became larger. Thus, larger decreases in blink gain accompanied increases in the density of c-Fos labeled neurons in the spinal trigeminal nucleus.

Plotting the average c-Fos labeled cell density in 640μm bins along the length of the trigeminal as a function of gain change revealed that rats with the largest gain decreases, <-0.2, had a higher density of c-Fos labeled cells compared to rats with smaller gain changes, >-0.2, ($F_{(1)}$= 75.976, p<0.001; *Figure 17A*). For rats with larger gain decreases (<-0.2), the highest density of c-Fos labeled cells occurred at the posterior

pole of the spinal trigeminal nucleus, approximately -17.8 mm caudal to bregma [140]. The minimum density of neurons occurred around -16 mm caudal to bregma, followed by a steady increase in the density of c-Fos labeled neurons toward the rostral end of the spinal trigeminal nucleus, approximately -10 mm caudal to bregma (Fig. 17A). The pattern of c-Fos labeled neurons in the rats with smaller gain changes (>-0.2) appeared similar except that the lowest density of labeling occurred -14.5 mm caudal to bregma. The average cell density of the entire ipsilateral spinal trigeminal nucleus was higher for large gain depression rats (<-0.2, 208 ± 57.7 cells/mm^2) than the average cell density for small gain change rats (>-0.2, 120.3 ± 28.3 cells/mm2; ($T_{(7)}$= 1.470, p >0.185 Fig. 17B). For comparison, the previously described averaged cell density data for HFS and No-HFS ipsilateral conditions were also plotted (*Figure 17B*).

c-Fos Cell Density as a Function of Gain Change in the Anterior and Posterior Termination Zones

When considered as a function of gain, there were significant differences between the low and high gain animals in the regions of SO termination within the trigeminal. The rats with larger gain decreases (<-0.2) exhibited a higher average density of c-Fos labeled cells at all levels compared to rats with smaller gain changes (>-0.2) in the anterior spinal trigeminal nucleus termination zone ($F_{(1)}$= 358.954, *p<0.001; Figure 18A*). The rats with largest gain decreases (<-0.2) showed a higher c-FOS cell density 209.9 ± 42.8cells/mm^2 than rats with smaller gain changes (>-0.2) 123 ± 31.8 cells/mm^2 in the anterior SO termination region ($T_{(7)}$= 1.649, *p=0.14; Figure 18B).* Similarly, rats with larger gain decreases (<-0.2) exhibited a higher density of c-FOS labeled cells compared to rats with gain changes (>-0.2) in the posterior SO termination zone ($F_{(1)}$= 297.197, *p<0.001; Figure 19A*). The rats with largest mean gain decreases showed a significant increase in c-FOS cell density 200.4 ±69.5cells/mm^2 compared to rats with smaller gain changes, 84.2 ± 29.3 cells/mm^2 in the posterior SO termination zone ($T_{(7)}$= 1.672, *p=0.14; Figure 19B).* Overall, the average c-Fos labeled cell density in the anterior SO termination zone, posterior SO

termination zone, and the entire spinal trigeminal nucleus followed a trend such that larger gain decreases accompanied higher c-FOS cell density (*Figures 18, 19*).

c-Fos Neuronal Activation in the Inferior Olive

Inferior olive activity is a key factor in eyelid conditioning and gain modification [142] [143] [144]. Neurons in the spinal trigeminal nucleus receiving SO stimulation innervate neurons in the contralateral IO (Fig. 4). Rats with larger gain decreases (<-0.2) had a higher density of c-Fos labeled cells in contralateral IO (42.5 ± 15.6 cells/mm^2) compared to rats with smaller gain changes (>-0.2; 16.8 ± 5.4 cells/mm^2), ($T_{(7)}$= -1.702, p=*0.13; Figure 20B)*. Plotting average c-Fos labeled neuron density as a function of condition, HFS vs. No HFS showed the same pattern as when separated by gain change ($T_{(7)}$= -1.225, p>*0.05; Figure 20B*). In the ipsilateral IO rats with larger gain decreases (<-0.2) exhibited a higher density of c-Fos labeled cells (44.2 ± 16.2 cells/mm^2) compared to rats with smaller gain changes (>-0.2; 24.0 ± 11.1cells/mm^2; *Figure 20A*) although this difference was not significant ($T_{(7)}$= -1.061, p > 0.05). Comparing average c-Fos labeled cell density based on HFS and No-HFS condition showed a similar result ($T_{(7)}$= -0.540, *p> 0.05; Figure 20A*. Although not statistically significant, the overall the average cell density (mm^2) as a function of gain change for the contralateral IO showed a strong trend toward an increased number of IO neurons predicting a larger gain change.

c-Fos Neuronal Activation in the Red Nucleus

The average cell density (mm^2) of c-FOS labeled cells within the ipsilateral and contralateral red nuclei also exhibited the pattern of higher cell density being associated with larger gain decreases. For the contralateral red nucleus, rats with larger gain decreases (<-0.2) had significantly more c-Fos activated cells (128.2 ± 30.6 cells/mm^2) compared to rats with smaller gain changes (>-0.2; 21.2 ± 8.5 cells/mm^2; ($T_{(3)}$= -

5.775, p<*0.05; Figure 21A*). Based on gain changes (>-0.2 and -<0.2), the RN ipsilateral to the SO stimulus showed a significantly higher density of c-Fos activated cells (112.9 ± 17.7 cells/mm^2) with larger gain decreases (<-0.2) when compared to rats with smaller gain changes (>-0.2; 40.7 ± 23.3 cells/mm^2; ($T_{(4)}$= -2.239, p<*0.05; Figure 21B*). Although the averages were similar when the data were separated based on condition, HFS vs. No-HFS, this difference was not significant ($T_{(4)}$= -0.589, *p> 0.05; Figure 21B*). Because c-Fos cell density data for two rats for the red nucleus contralateral to the SO stimulus were lost, the same rats were in the HFS and the >-0.2 groups, data were only plotted based on gain change (Fig. 21A).

c-Fos labeled Cell Density as a Function of Change in Excitability

Modifications in blink reflex excitability accompanied changes in blink reflex gain (Fig.22). With larger decreases in blink reflex gain, there was a significant increase in the excitability of reflex blinks measured by the ratio of the amplitude of the 2nd blink divided by the amplitude of the 1st blink in the paired stimulus paradigm between the pre and post blocks regardless of condition (n=9, r=-.713, p <0.05; Fig. 22). This relationship indicated that c-Fos labeled cell density in spinal trigeminal nucleus might predict changes in blink reflex excitability pre and post. There was a significant correlation between the c-Fos labeled cell density over the entire spinal trigeminal nucleus and increased reflex blink excitability from pre to post blocks regardless of treatment condition (n=9, r =.823, p <0.05; Fig. 23). The density of c-Fos labeled cells in the anterior (Fig. 24A) and posterior (Fig. 24B) SO termination zones also predicted the change in reflex blink excitability from pre to post blocks. These correlations were significant for the anterior (n=9, r =.708, p <0.05;Fig. 24A) termination zone, and significant for the posterior termination zone (n=9, r =0.801, p <0.05;Fig. 24B). Overall these data showed that increases c-Fos labeled cell density in the spinal trigeminal nucleus predicted increased changes in reflex blink excitability following HFS or No-HFS treatment.

Summary of c-Fos Cell Density in the Trigeminal Blink Reflex Circuit

When rats were separated by large or small gain changes, the spinal trigeminal nucleus, inferior olive and the red nucleus demonstrated a strong and similar trend. The higher c-Fos cell density, the larger the gain change in each region (Fig.25). The spinal trigeminal nucleus sends excitatory input to the contralateral inferior olive. The average c-Fos cell density in the contralateral inferior olive was higher for rats with a large gain decrease than rats with a small gain decrease. The neurons in the inferior olive send excitatory projections to the cerebellar cortex and the interpositus nucleus in the cerebellum. The interpositus nucleus projects to the contralateral red nucleus. The average cell density in the contralateral red nucleus was higher in rats with large gain change than rats with small gain change. Overall the spinal trigeminal nucleus, inferior olive and red nucleus c-Fos cell density followed a similar trend, higher c-Fos cell density the larger the gain decreases.

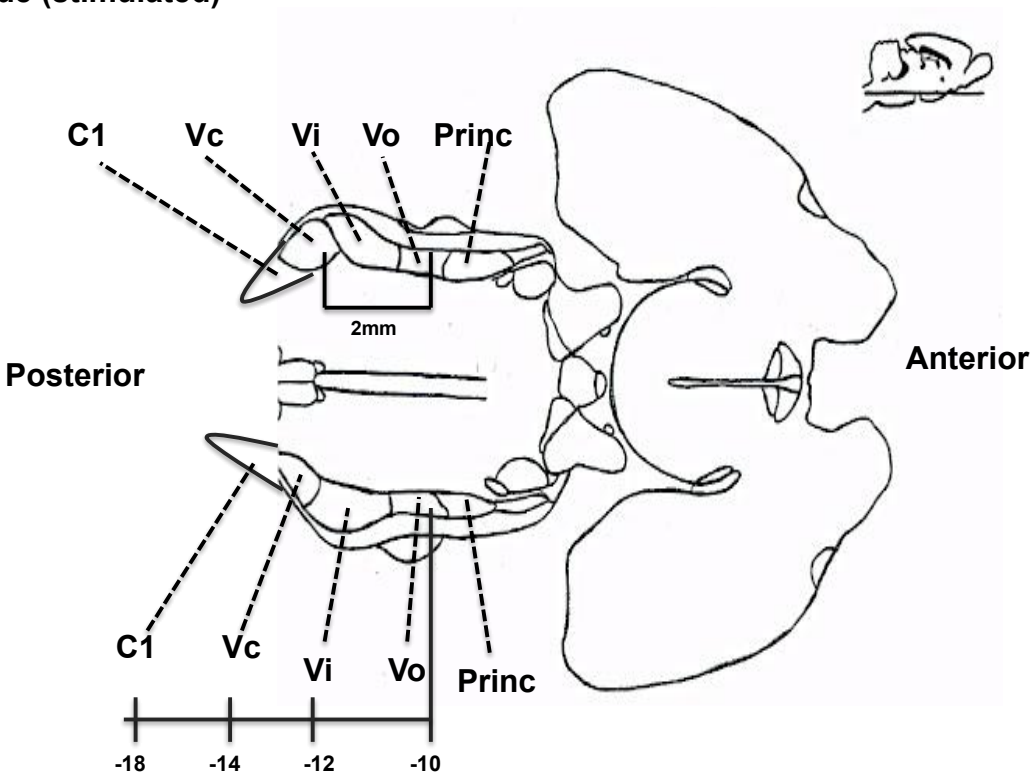

Fig. 9. Horizontal section (DV: 8.82mm) of a rat brain taken from Paxinos Atlas [140] showing the spinal trigeminal complex and cervical one of the spinal cord and stereotaxic coordinates relative to bregma Abbreviations: C1, cervical 1; Princ, Principal spinal trigeminal nucleus; Vc, caudalis subdivision of spinal trigeminal nucleus; Vi, interpolaris subdivision of spinal trigeminal nucleus; Vo, oralis subdivision of spinal trigeminal nucleus;

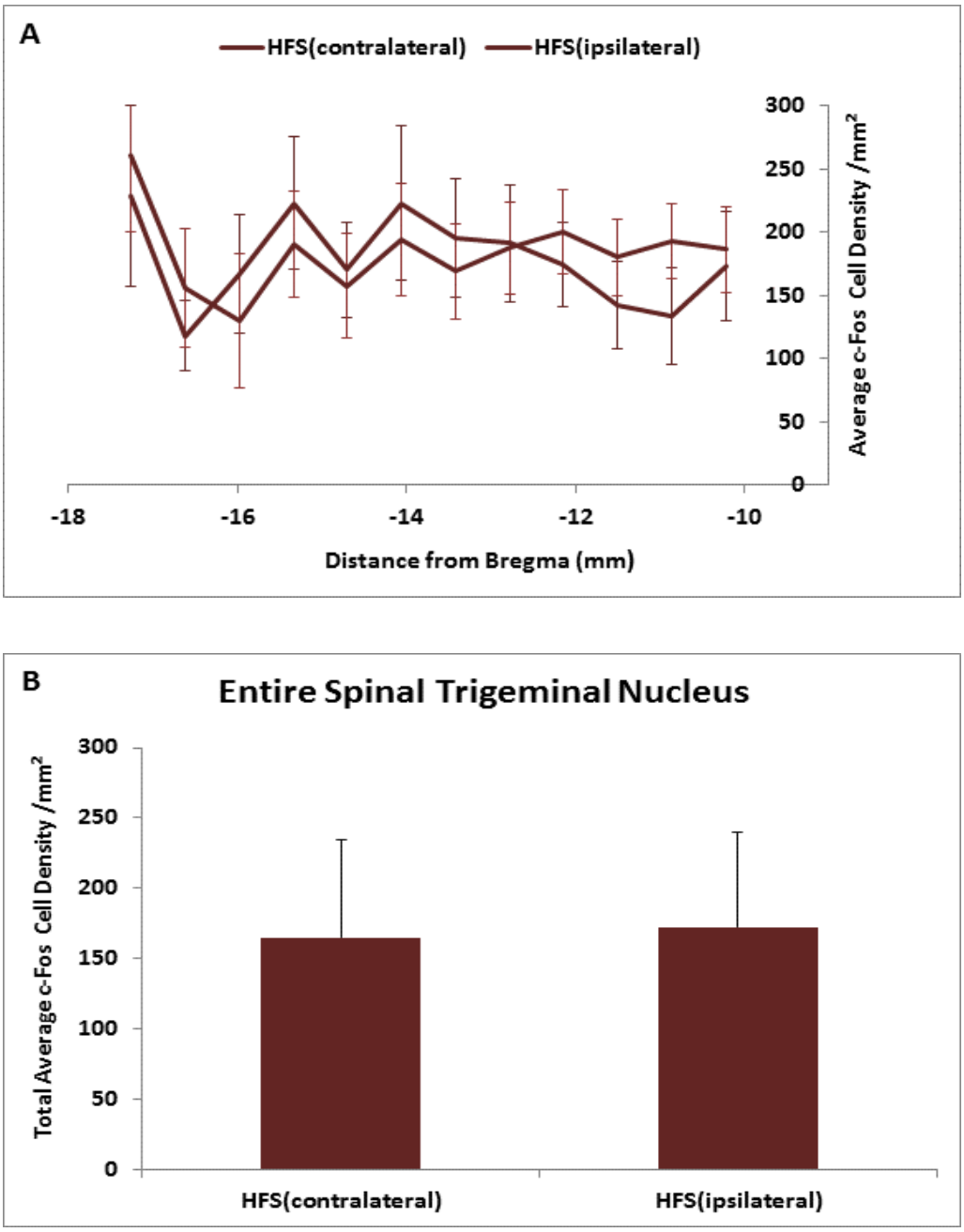

Fig. 10. Density of c-Fos labeled cells within the spinal trigeminal nucleus of rats receiving HFS. **(A)** Average cell density/mm^2 in c-Fos neurons in 640 µm bins along the length of the spinal trigeminal nucleus for the stimulated trigeminal (HFS (ipsilateral)) and unstimulated side (HFS (contralateral)). **(B)** Average cell density of c-Fos neurons within the entire spinal trigeminal nucleus for the stimulated trigeminal (HFS (ipsilateral)) and unstimulated trigeminal (HFS (contralateral)). Error bars are SEM.

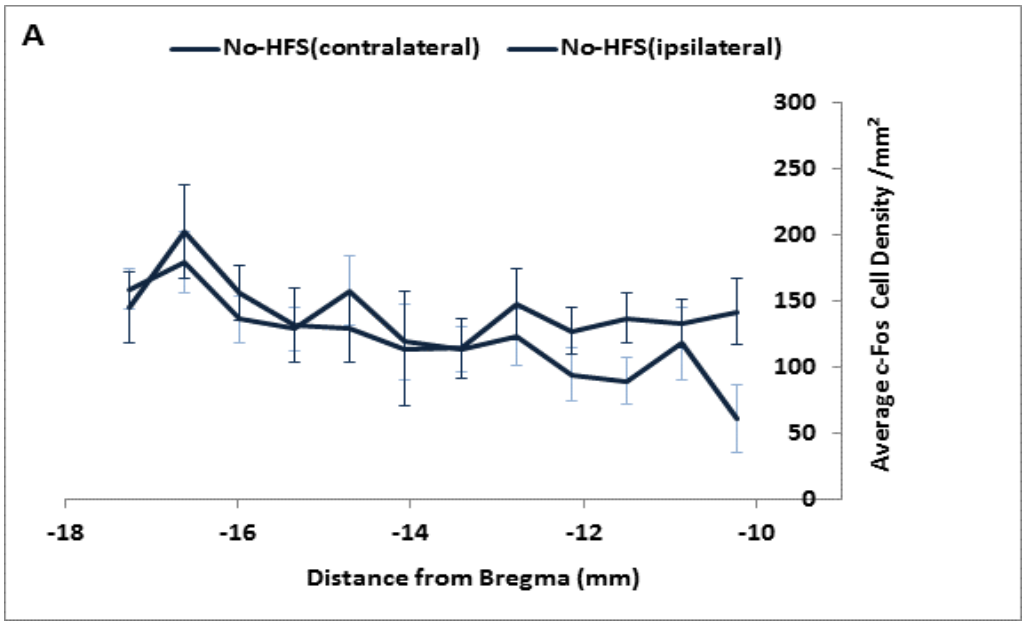

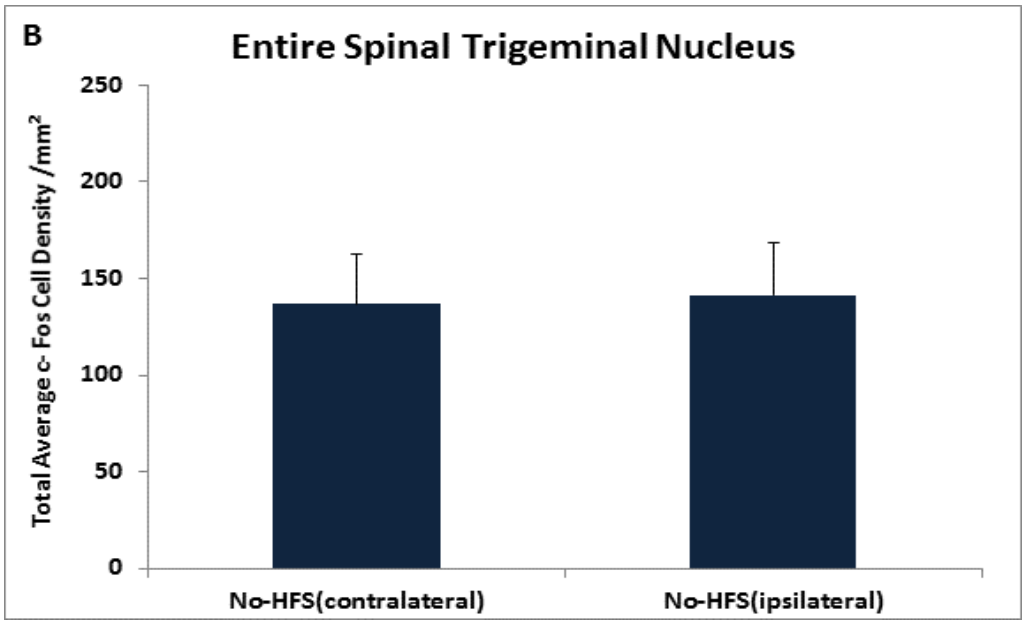

Fig. 11. c-Fos labeled cells within the spinal trigeminal nucleus of rats receiving No-HFS treatment. **(A)** Average cell density/mm^2 in c-Fos neurons in 640 µm bins along the length of the spinal trigeminal nucleus for the stimulated trigeminal (No-HFS (ipsilateral)) and unstimulated side (No-HFS (contralateral)). **(B)** Average cell density of c-Fos neurons for the spinal trigeminal nucleus for the stimulated (No-HFS (ipsilateral)) and unstimulated sides (No-HFS (contralateral)). Error bars are SEM.

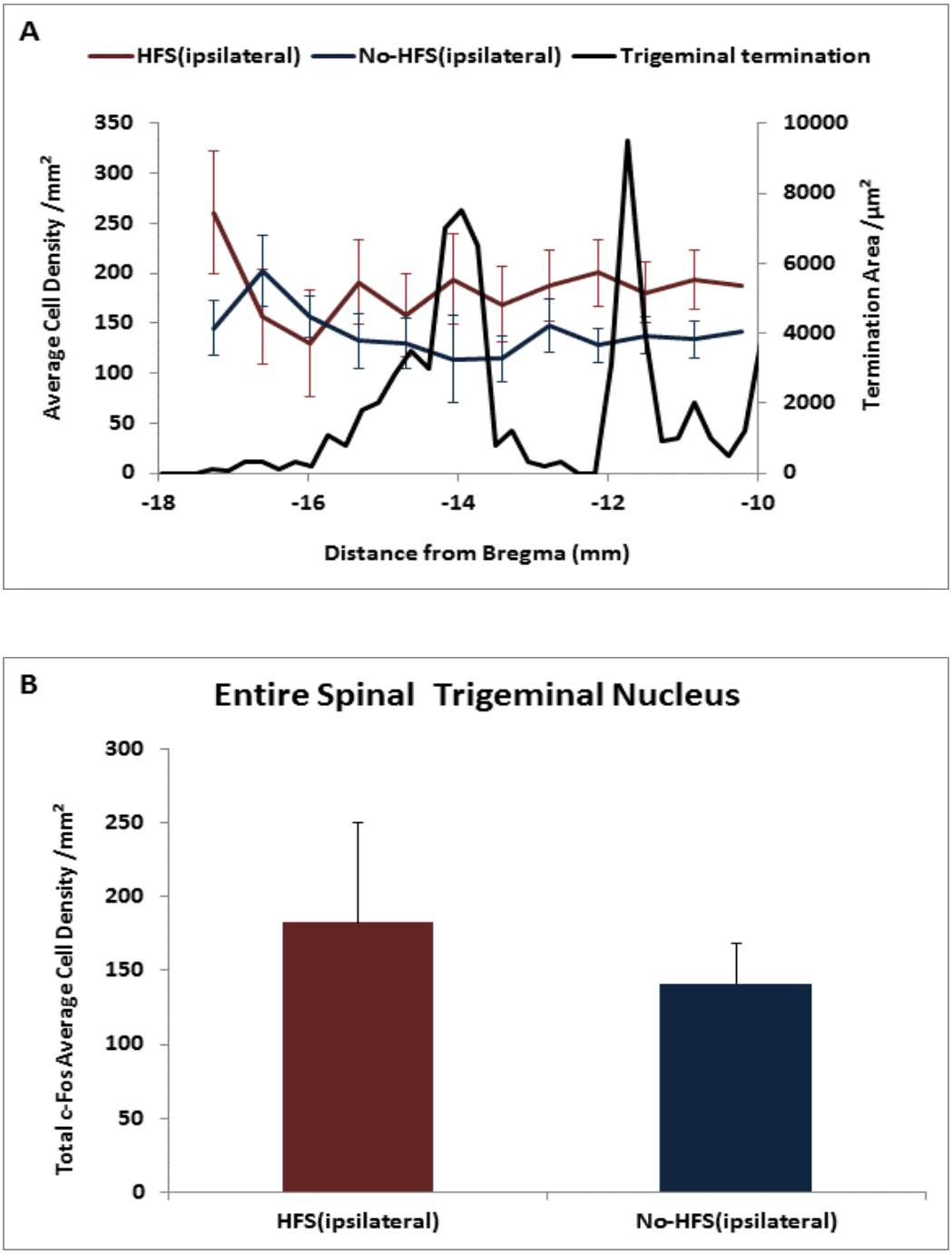

Fig. 12. Comparison of c-Fos density for rats receiving HFS or No-HFS stimulation. **(A)** Average cell density/mm^2 of c-Fos neurons in 640 µm bins along the length of the spinal trigeminal nucleus for rats in the HFS paradigm (HFS (ipsilateral) or No-HFS paradigm (No-HFS (ipsilateral). Black trace shows the area of supraorbital nerve termination µm^2 based on Gong et al., 2003 [31]. **(B)** Average cell density/mm^2 of c-Fos neurons for the spinal trigeminal nucleus for rats receiving HFS (HFS (ipsilateral)) and No-HFS (No-HFS (ipsilateral)). Error bars are SEM.

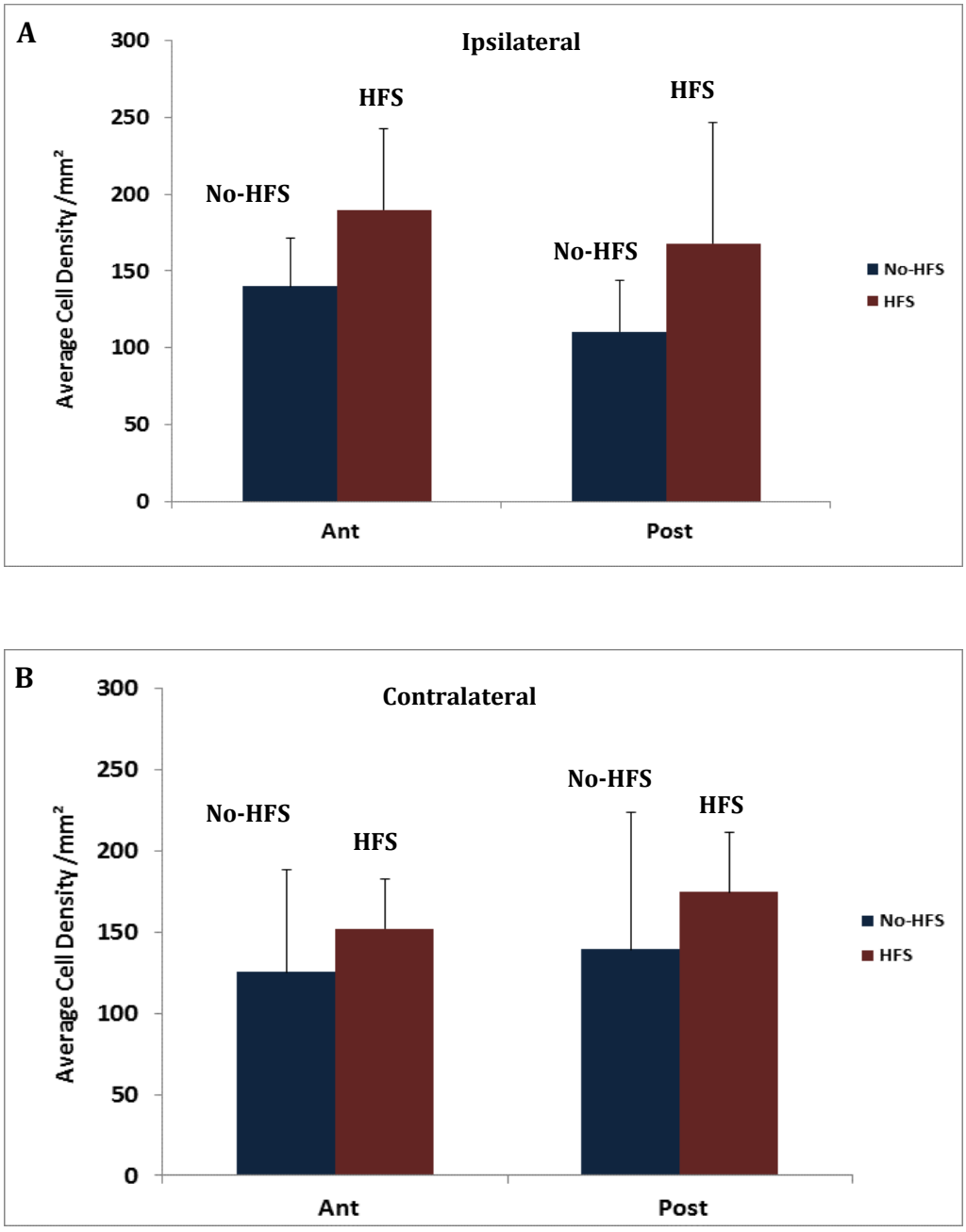

Fig. 13. Average c-Fos labeled cell density/mm^2 in the anterior (Ant) and posterior (Post) termination zones of the supraorbital nerve within the spinal trigeminal nucleus for rats receiving HFS and No-HFS. **(A)** Average cell density in the spinal trigeminal nucleus receiving stimulation. **(B)** Average cell density for the unstimulated spinal trigeminal nucleus. Error bars are SEM.

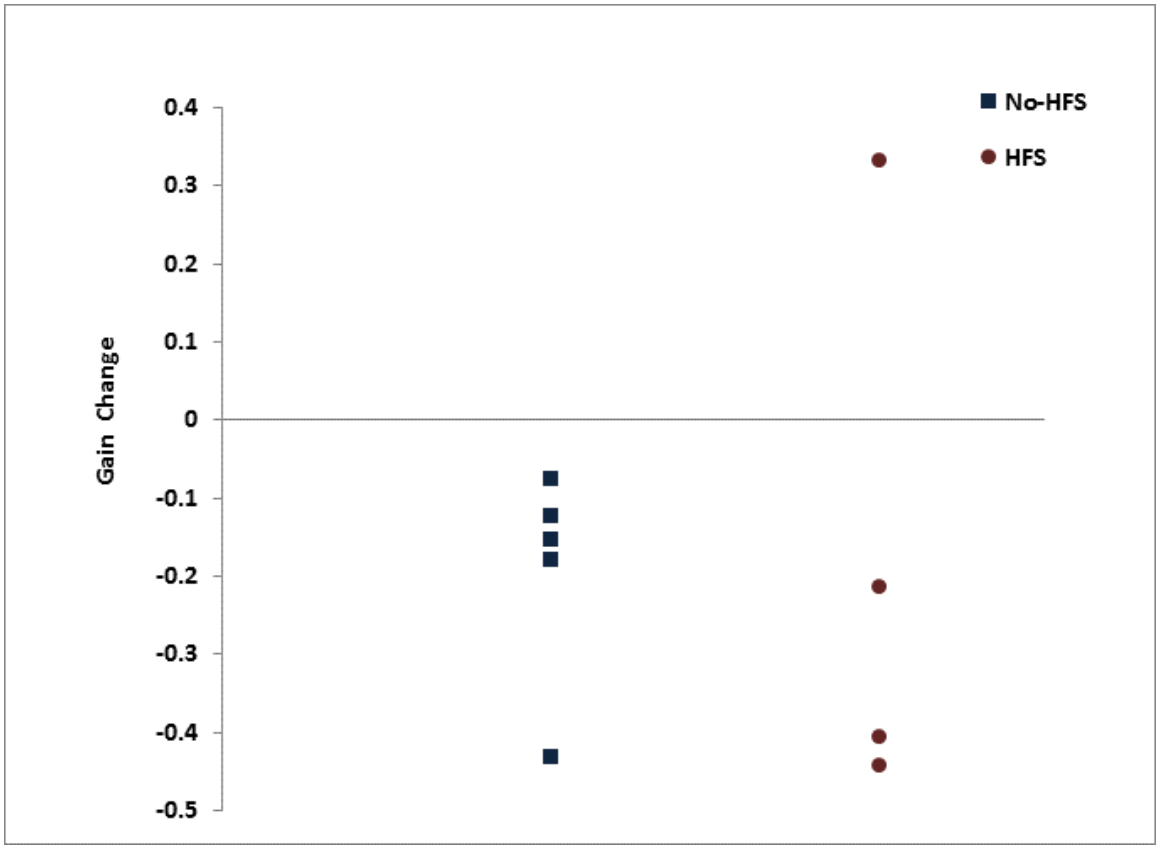

Fig. 14. Gain changes with HFS and No-HFS treatment. Each point is an individual rat.

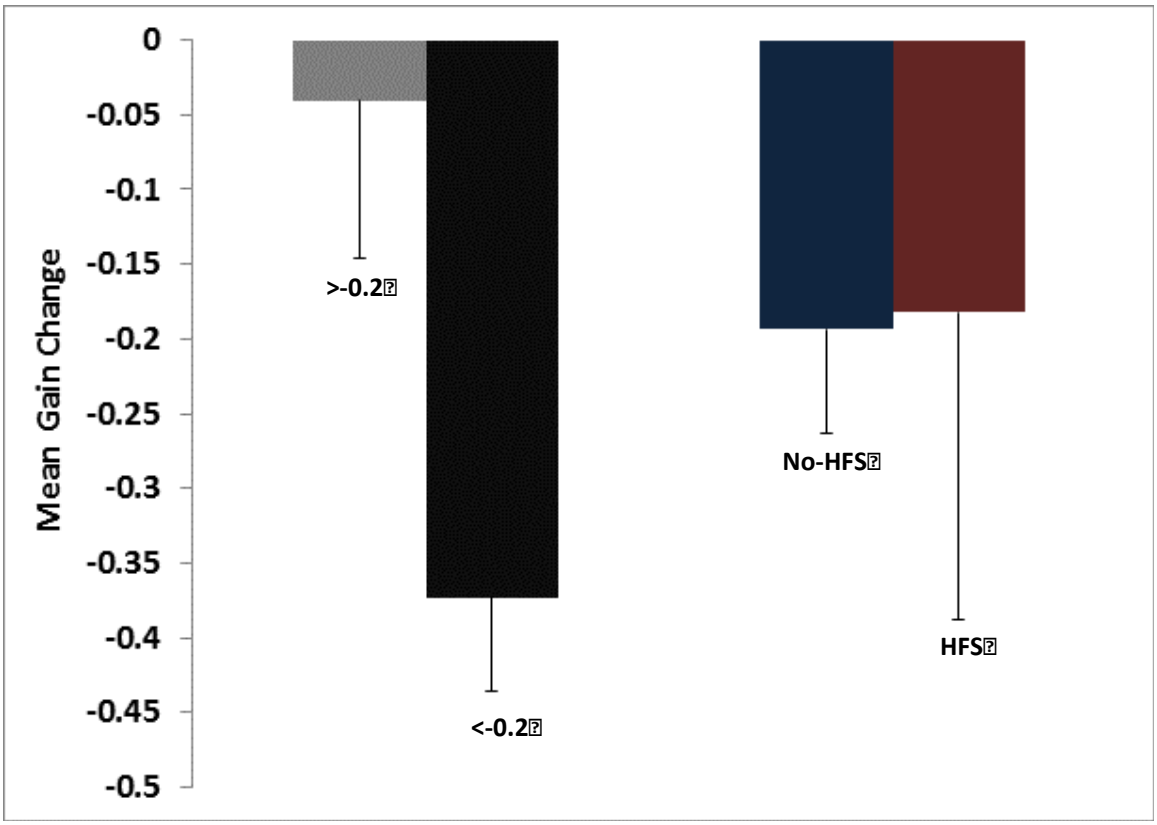

Fig. 15. Average gain change by condition (No-HFS and HFS) and average gain change for the same rats sorted by magnitude of gain change <-0.2 and >-0.2 independent of treatment condition. *p<0.05. Error bars are SEM.

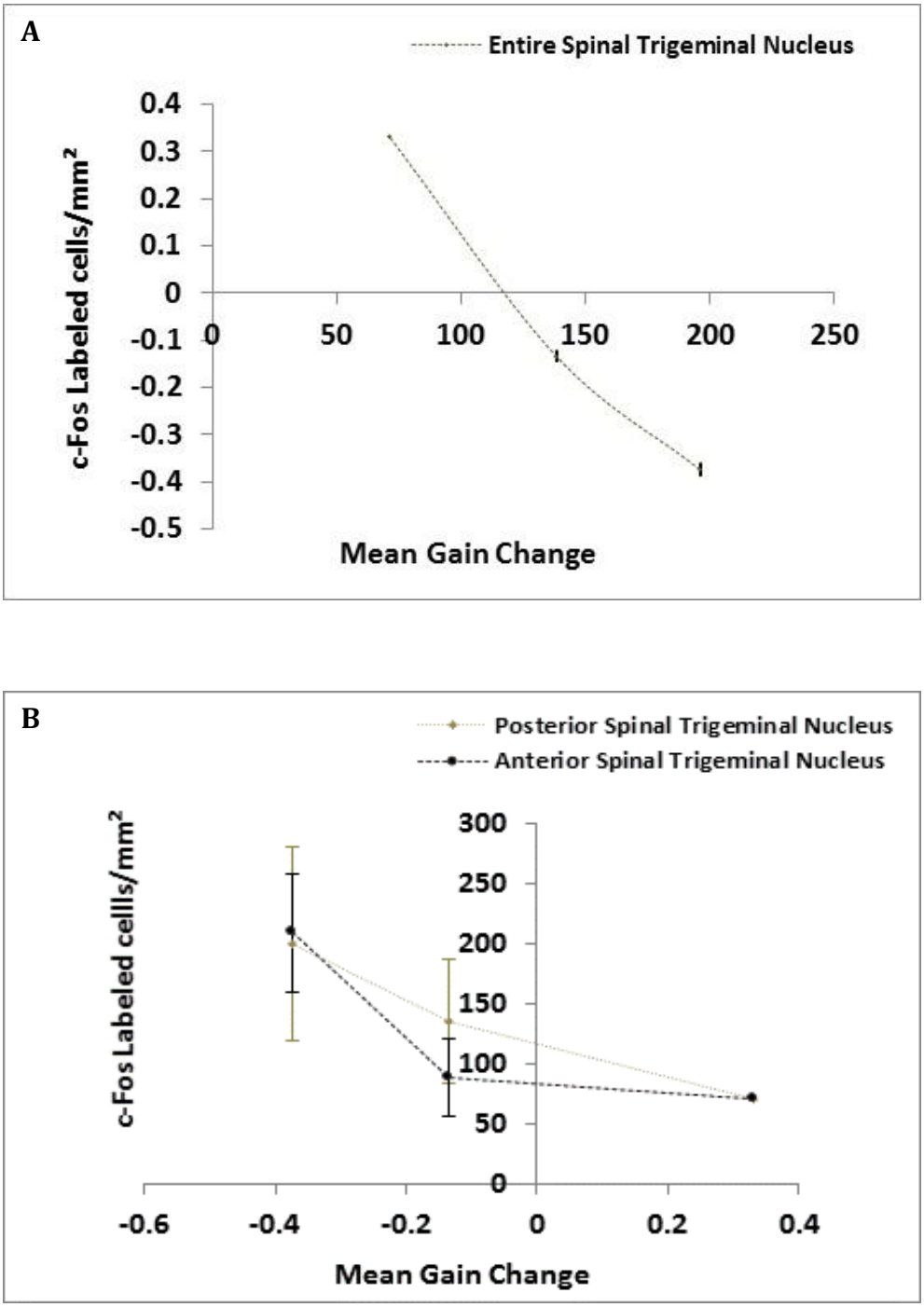

Fig. 16. Average c-Fos labeled cell density in the spinal trigeminal nucleus as a function of mean gain change for the **(A)** entire spinal trigeminal nucleus, **(B)** anterior supraorbital termination zone (●) and posterior supraorbital termination zone (◆).Error bars are SEM

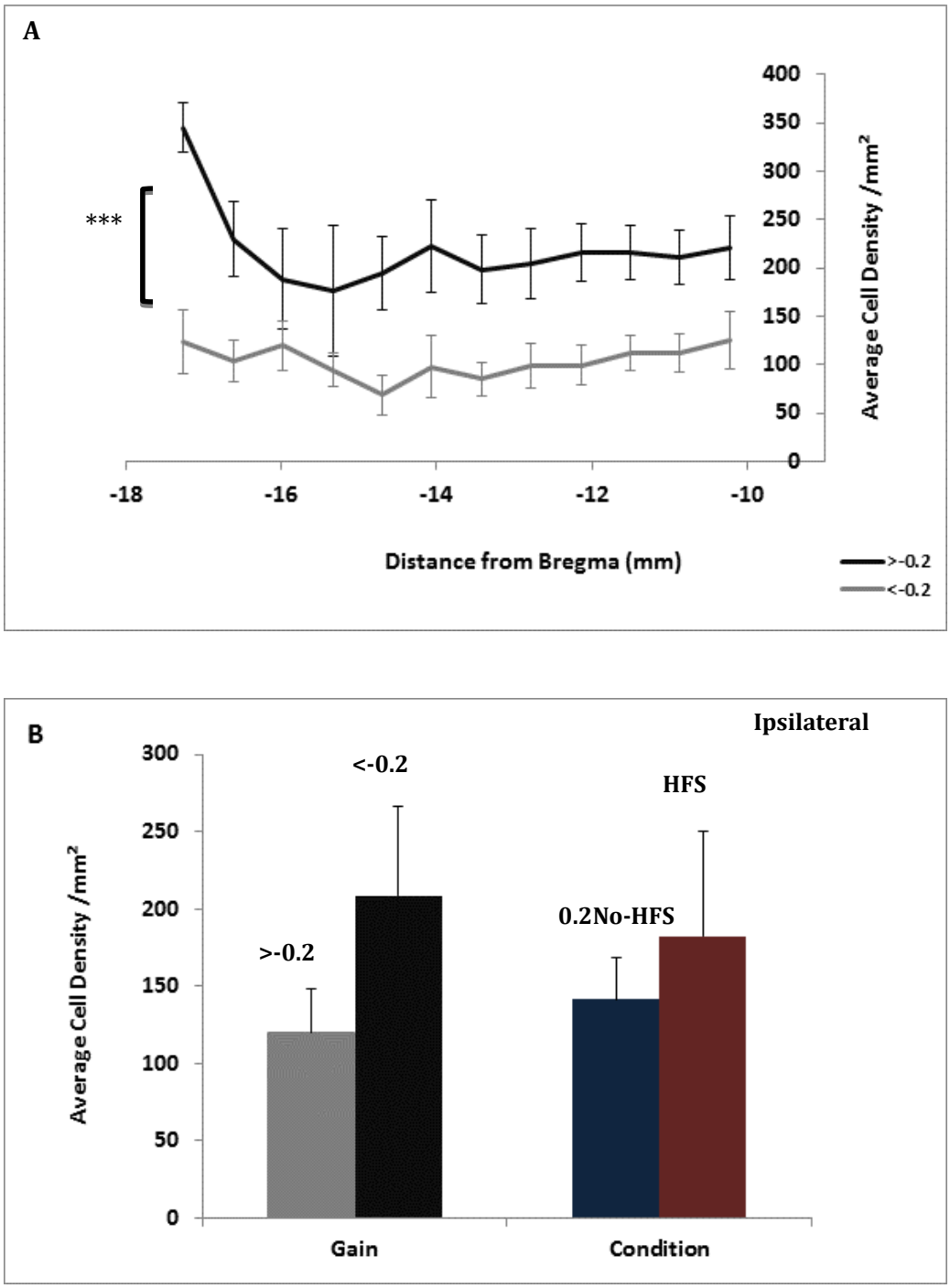

Fig. 17. Average c-Fos labeled cell density throughout the spinal trigeminal nucleus. **(A)** Average cell density/mm^2 of c-Fos neurons in 640 µm bins along the length of the spinal trigeminal nucleus for rats with gain changes < -0.2 (black line) and gain changes >-0.2 (gray line). **(B)** Average cell density for the entire spinal trigeminal nucleus with gain changes (>-0.2 and <-0.2) and condition (HFS and No-HFS). *** $p < 0.001$. Error bars are SEM.

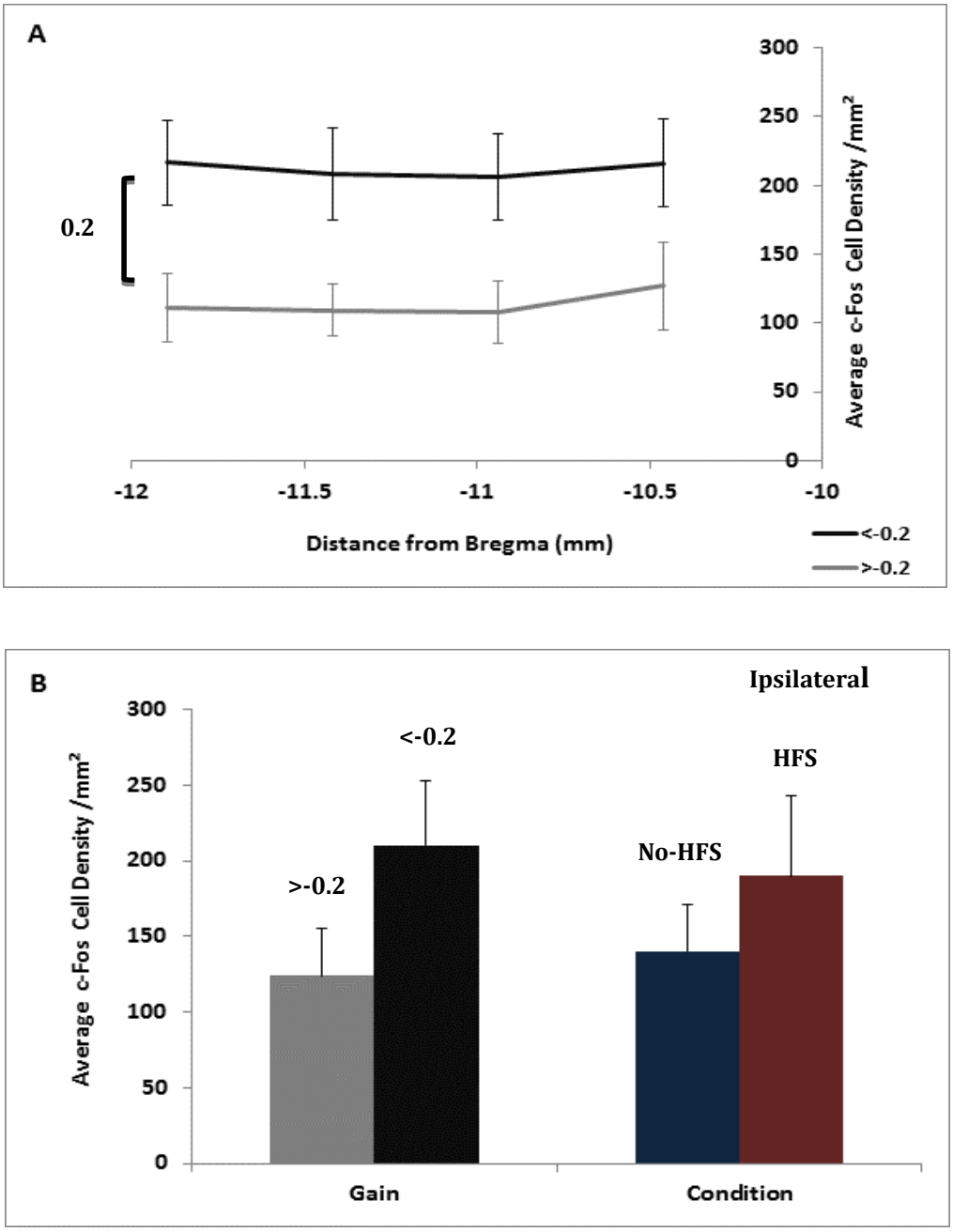

Fig. 18. Average c-Fos cell density in the anterior supraorbital nerve termination zone. **(A)** Average cell density/mm^2 of c-Fos neurons in 640 µm bins through the anterior SO termination zone for rats with gain changes < -0.2 (black line) and gain changes >-0.2 (gray line). **(B)** Average cell density for the anterior supraorbital termination zone with gain changes (>-0.2 and <-0.2) and condition (HFS and No-HFS). *** $p < 0.001$. Error bars are SEM.

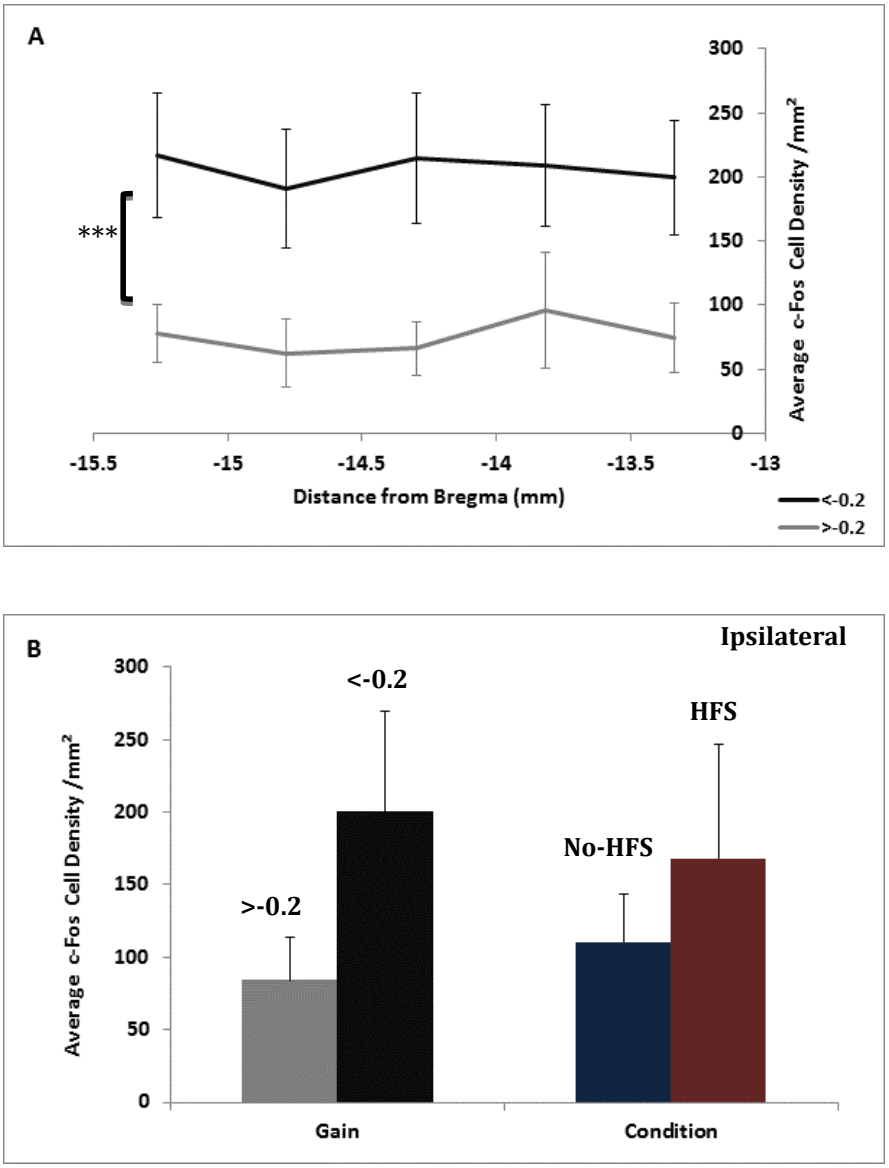

Fig. 19. Average c-Fos cell density in the posterior supraorbital nerve termination zone. **(A)** Average cell density/mm^2 of c-Fos neurons in 640 µm bins through the posterior SO termination zone for rats with gain changes < -0.2 (black line) and gain changes >-0.2 (gray line). **(B)** Average cell density for the posterior supraorbital termination zone with gain changes (>-0.2 and <-0.2) and condition (HFS and No-HFS). *** $p < 0.001$. Error bars are SEM.

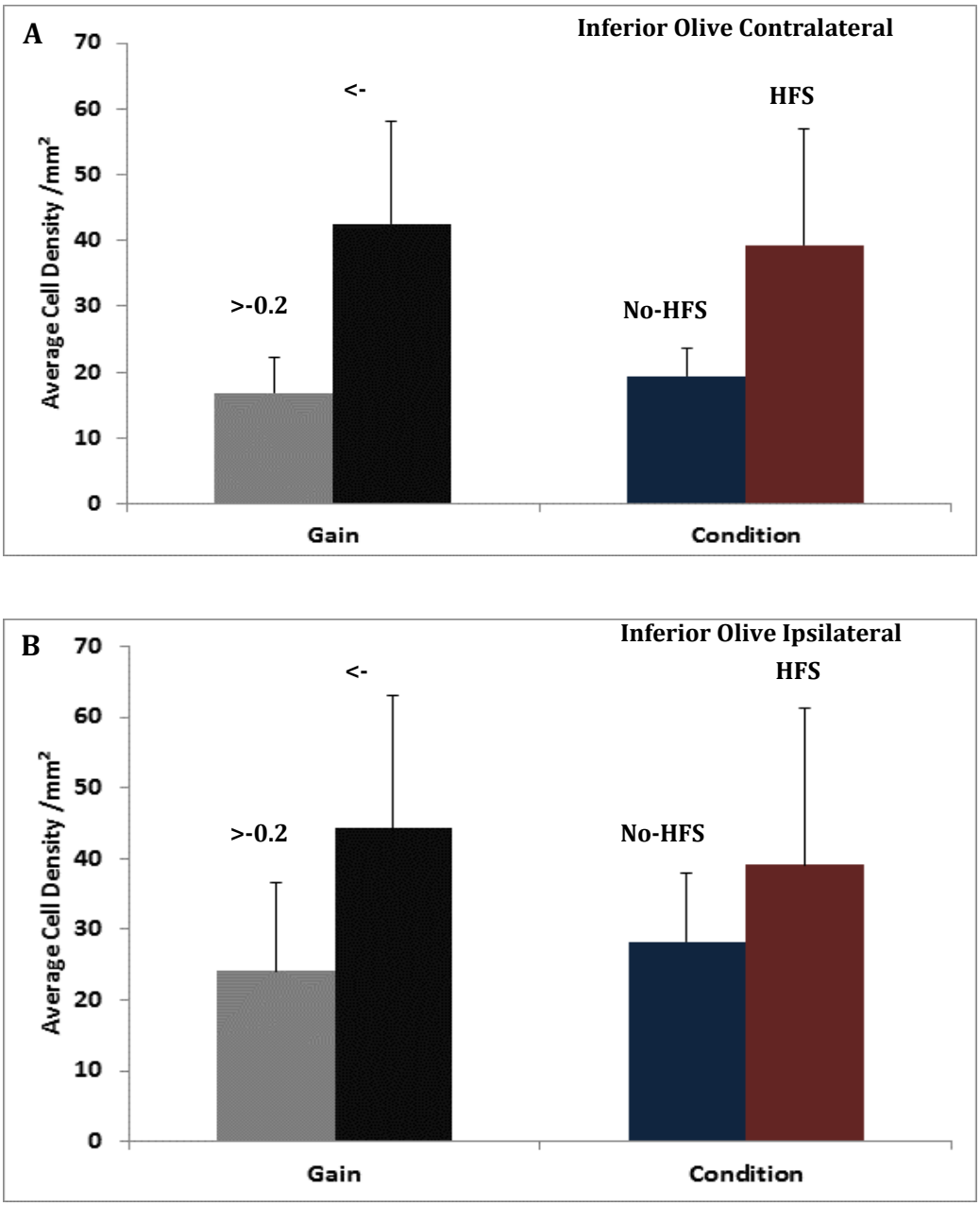

Fig. 20 Average c-Fos labeled cell density/mm^2 in the inferior olive based on gain changes (<-0.2 and >-0.2) and condition (HFS and No-HFS) for the IO contralateral (A) and ipsilateral (B) to supraorbital stimulation. Error bars are SEM.

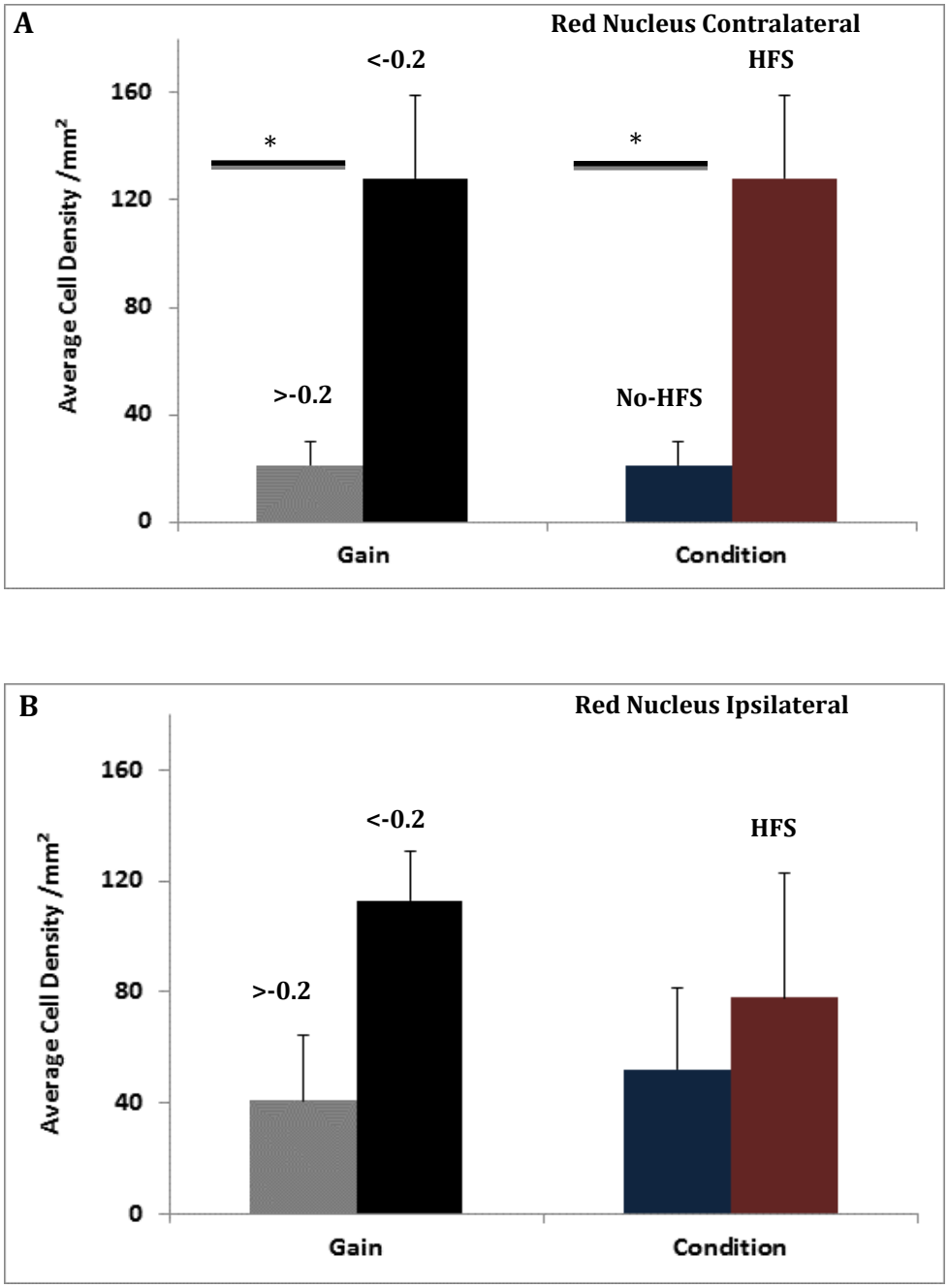

Fig. 21 Average c-Fos labeled cell density/mm^2 in the red nucleus with gain changes (<-0.2 and >-0.2) and condition (HFS and No-HFS) for the red nucleus contralateral (A) to the supraorbital stimulus and gain change plotted for red nucleus ipsilateral (B) to the supraorbital nerve stimulation. *p <0.05**.** Error bars are SEM.

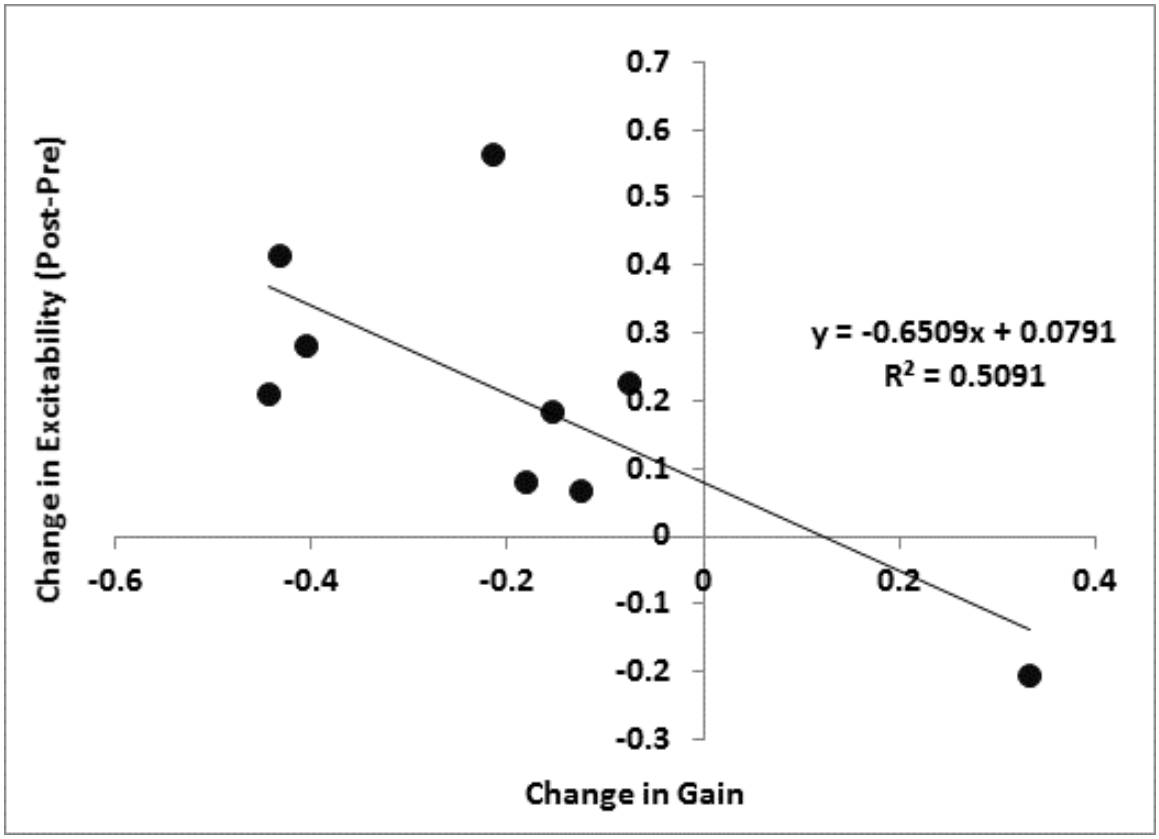

Fig. 22. Change in the excitability of the trigeminal reflex blinks from Pre to Post as a function of gain change in the entire spinal trigeminal nucleus for each rat.

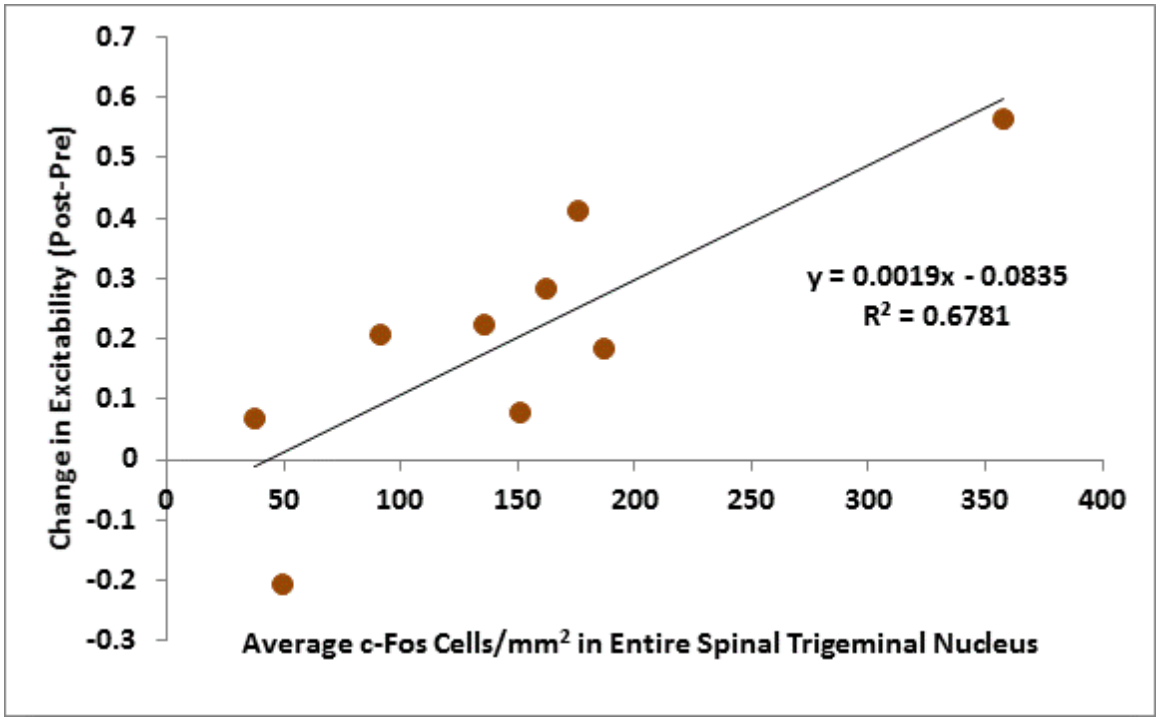

Fig. 23. Change in the excitability of the trigeminal reflex blinks from Pre to Post as a function of average c-Fos labeled cell density/mm^2 in the entire spinal trigeminal nucleus. Each point is an individual rat.

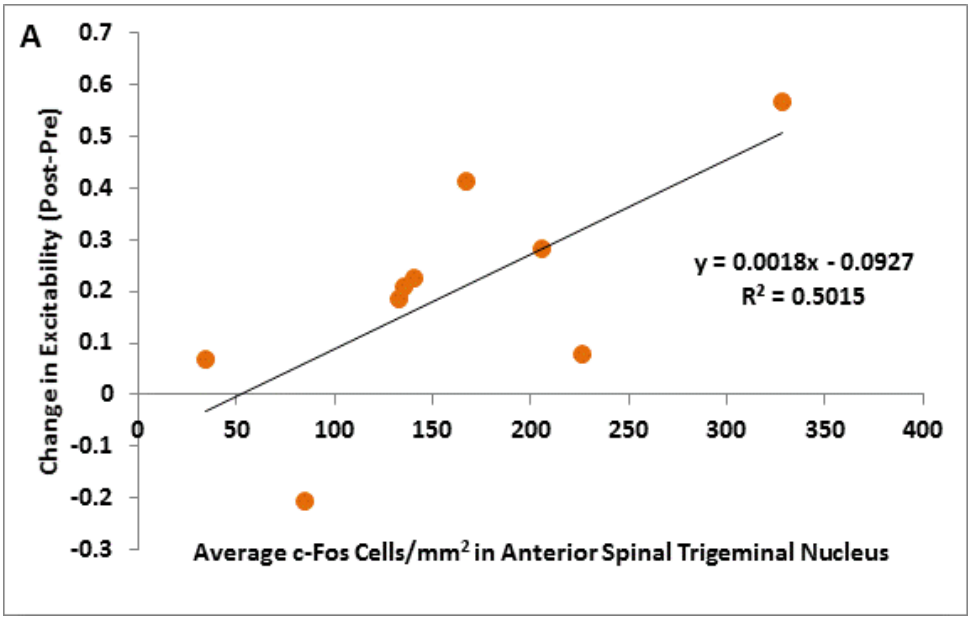

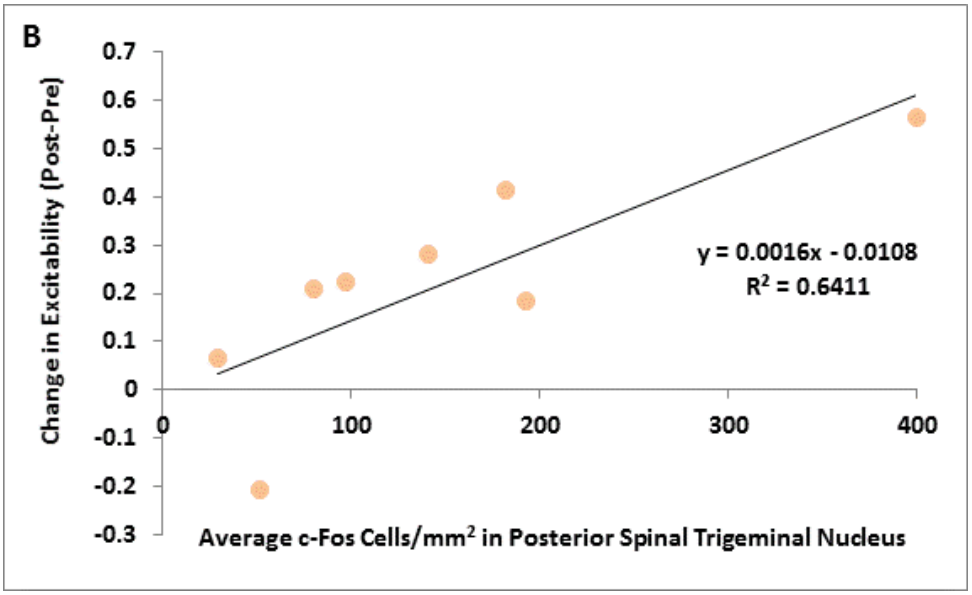

Fig. 24. Change in the excitability of the trigeminal reflex blinks from Pre to Post as a function of average c-Fos labeled cell density/mm^2 in (A) the anterior termination zone of the supraorbital nerve and (B) the posterior SO termination zone). Each point is an individual rat.

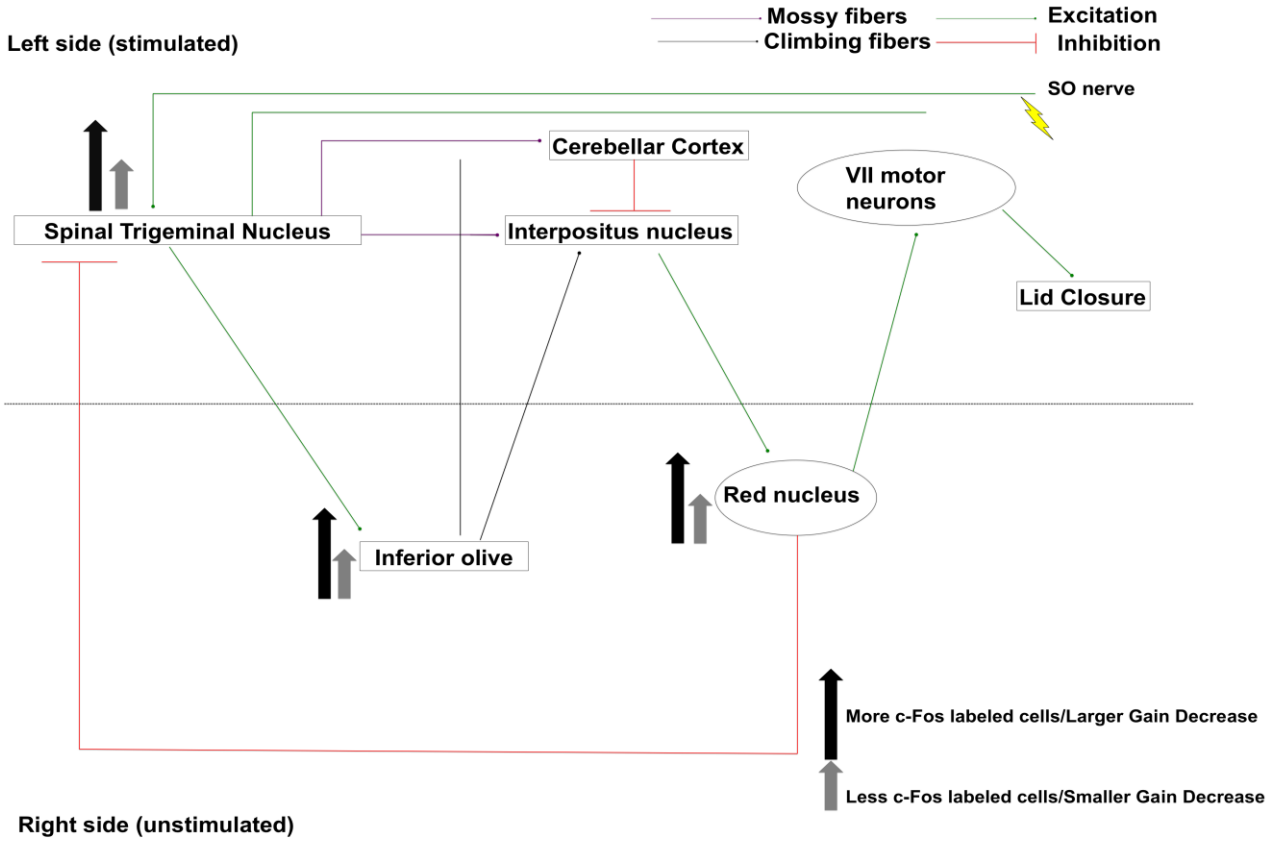

Fig. 25. Summary of Circuit diagram of the cerebellum and the spinal trigeminal nucleus connections involved in trigeminal reflex blinks during Gain Changes

Discussion

My experiments utilized the blink system to investigate neuronal activation with either HFS-B or a single supraorbital nerve stimulus. The goal of these experiments was to determine the distribution of neurons activated by HFS training that decreased the gain of the trigeminal reflex blink in addition to those activated by SO stimulation alone.

c-Fos Immunohistochemistry: Advantages and Disadvantages

c-Fos immunohistochemistry is the technique used to determine neuronal activation in these experiments. The immediate early gene c-Fos is a marker used to measure changes in gene expression cause by neuronal activation [130] [131] [132] [133, 145] [146] There are advantages and disadvantages to using c-Fos as a neuronal activity marker. One advantage is that c-Fos immunohistochemistry allows the identification and comparison of neuronal cell activation in different brain regions. Like most things, c-Fos has its limits. The first limit of c-Fos expression is it may be turned on by a wide variety of signaling pathways. The different signaling pathways can be activated by environmental cues or even stress that may activate more c-Fos cells in the region of interest. For example, c-Fos expression alone cannot provide much information about the signaling pathways involved. Next c-Fos expression does not indicate whether the activation of a neuron is due to direct or indirect effects. The stimulation paradigm used in our lab is designed to stimulate the SO nerve specifically. It is possible, however, that stimulation of the SO nerve may activate brain regions other than the trigeminal blink reflex circuit. This may lead to indirect neuronal activation of other pathways that may send an input to any brain region within the trigeminal blink reflex circuit. This possibility may influence the number of labeled cells observed in the trigeminal reflex blink

circuit. Lastly, even though c-Fos can mark inhibitory neurons, it is most useful in measuring activation rather than inhibition[123] [145] [147]. Therefore in future experiments, it is critical to double label to mark inhibitory neurons. This approach may help to determine whether HFS-B increases the activity of inhibitory neurons. Despite the limitations of c-Fos, it is a commonly used method of assessing neuronal activation. By using c-Fos immunohistochemistry, it is possible to look at different populations of activated neurons in the HFS and No-HFS conditions. The c-Fos immunohistochemistry technique also allows comparison of the quantity of labeled c-Fos cells as function of gain change.

Gain Changes in Spinal Trigeminal

Based on previous data, HFS modulation of the trigeminal blink reflex caused gain changes [108] [139] [107]. In this study, rats with a large gain change demonstrated a higher density of c-Fos cell activation than rats with smaller gain changes (Fig 16-19). However, in Figure 15 both the HFS and No-HFS conditions have extreme value outliers. These extreme values provide insight about gain changes for two reasons. The first reason is, if supraorbital nerve damage occurred during surgery this may contribute to the extreme values in the HFS and No-HFS conditions. Assuming that I damaged the nerve, this could affect or disrupt nerve function. Trigeminal nerve damage usually produced an excitability increase from pre to post damage [148]. After analyzing the excitability data for each rat (Fig 22), the No- HFS rat with extreme gain change (-0.43) exhibited an excitability increase. The HFS rat with an extreme gain change (0.33) did not show an excitability increase. **Secondly**, the HFS or No-HFS extreme values may influence the number of c-Fos cells in the ipsilateral and contralateral trigeminal. The one No-HFS rat that showed more c-Fos labeled cells activated with a large gain decrease may have influenced the average cell density in the No-HFS condition. Therefore the No-HFS and HFS condition may not demonstrate any significant difference in the number of c-Fos labeled cells in average cell density data.

c-Fos Neuronal Activation in the Anterior and Posterior Spinal Trigeminal Nucleus

The quantity of c-Fos labeled cells in the anterior and posterior SO termination zones [19] [31] within the spinal trigeminal nucleus was analyzed as a function of gain change because neurons in the different subnuclei of the spinal trigeminal nucleus may have different roles. Neurons located in the anterior subdivision in rat project directly to orbicularis oculi motoneurons [49] [48, 50] [19, 51]. Damaging the anterior region impaired cornea-evoked blinks in humans [149]. Cornea evoked blink is an involuntary closure of the eyelids elicited by electrical or mechanical stimulation of the cornea. Unlike the blink reflex evoked by SO stimulation, corneal stimulation evoked only one OO response [51] [104] [105] [21]. The latencies for these responses are similar to the latencies for R2 component in SO stimulation [51, 150] [21] [20] . There are several lines of evidence that demonstrated the corneal afferent fibers terminate in the anterior and posterior SO termination regions of the spinal trigeminal nucleus [32, 151] [33] [152]. Physiological data indicated that corneal evoked blinks might activate posterior inhibition of anterior trigeminal blink reflex neurons [153-155] [156]. Therefore damage to posterior trigeminal region can alter the corneal blink reflex. Damaging the posterior SO termination zone in guinea pig trigeminal complex eliminated the R2 response [19]. The contribution of inhibitory neurons in the anterior or posterior terminations zones of the SO to the SO evoked reflex blink circuit is unknown. Based on previous data on the corneal evoked blink on the neurons in anterior and posterior trigeminal termination zones, it is possible that the neurons in anterior and posterior may be contributing to the overall depression within circuit. The current gain change data suggest that the neurons in the anterior and posterior end of the trigeminal maybe driving the depression produced by the HFS-B paradigm. The anterior neurons initiated the orbicularis oculi motoneurons discharge for SO evoked blinks [19] and corneal reflex blinks [51], whereas stimulation of neurons in the posterior termination zone suppressed the corneal reflex blink [153]. The current data showed that rats with a large gain change exhibited more cells in both the anterior and posterior regions of the spinal trigeminal nucleus (Figs. 18, 19). Comparing the c-Fos labeled cell density in the anterior to the posterior spinal trigeminal nucleus for rats with large gain decreases, the anterior and posterior region exhibited a

similar density of labeled c-Fos cells. Based on the gain change results, it is possible that both regions may be contributing equally to the depression in the trigeminal reflex blink circuit. It is unclear from these data if the neurons in the anterior and posterior are primarily inhibitory. Nevertheless Avendano [157] demonstrated through immunocytochemical and stereological analysis that approximately one-third of cells in the caudalis subdivision of the spinal trigeminal nucleus are inhibitory. This group also showed that one-third of cells in the interpolaris subdivision are inhibitory. Based on this evidence, maybe a small population of inhibitory neurons in the caudalis and interpolaris may be sufficient to drive the depression in the spinal trigeminal nucleus. In contrast to the gain change data that was previously mentioned, the HFS and No-HFS conditions did not demonstrate any significance difference in c-Fos activated cells (Figs. 18, 19). The small number of animals in this study may explain this lack of significance and be applicable to all of the statistics, not only the HFS and No-HFS condition data. Perhaps the spinal trigeminal nucleus and IO data would be significant if more animals were in the study. Although the small number of rats may influence the data, there are other possible explanations that may impact the number of c-Fos cells activated in the IO and RN data.

c-Fos Neuronal Activation in the Inferior Olive

One possibility that may influence the neurons in the IO is that the IO receives many inputs other than the trigeminal. The inferior olive receives inputs from the contralateral spinal trigeminal nucleus [54-56]. The immunohistochemical findings in this study indicate that when rats receive either HFS-training or No-HFS, the quantity of c-Fos cells activated in the inferior olive shows no significant difference between the two conditions. Because there are multiple inputs to the IO, the data may show no significant difference in the c-Fos labeled cells. These other inputs to IO may influence the number of c-Fos cells activated in the IO during the HFS and No-HFS conditions. For example, an anatomical experiment in cats demonstrate some neurons in the dorsal column and pretectum project to the IO [158]. The pretectum receives sensory

information from retinal ganglions cells in both eyes. Bull et al (1990) explain that the projections from the dorsal column and pretectum predominantly terminate in the dorsal inferior olive [158]. It's unknown if the neurons that project from these regions to the IO target the same neurons as spinal trigeminal nucleus. There is no direct evidence in the current study to show that the pretectum and dorsal column nuclei are active during HFS/No-HFS treatment. The stimulation paradigm in this study stimulates the SO branch of the trigeminal nerve. This sends an excitatory input to the neurons in IO. Neurons in the inferior olive are electrically coupled by gap junctions [159] [160] [161] [162] [163] [164] [165]. The distribution and properties of gap junction have been studied intently [159] [160] [161] [162] [163] [164] [165]. The IO neurons could couple to neighboring neurons at different synaptic strengths. This coupling mediates the synchrony of neurons in the IO [159] [160] [161] [162] [163] [164] [165]. It is possible for crosstalk to occur among neurons in the IO. If during the HFS or No-HFS treatment there is crosstalk among neurons this can trigger activating or inactivating nearby neurons. This crosstalk among neurons could potentially affect neuronal activation during HFS or No-HFS condition. The spinal trigeminal nucleus sends most of its projections to the dorsal inferior olive [56, 166] [55] [54]. Another possibility is if overlapping occurs, then some of the same neurons in the dorsal IO receive input from the spinal trigeminal nucleus, pretectum and dorsal column. This is a possibility if HFS or No-HFS treatment also activates the pretectum and dorsal column nuclei. Another possibility that may occur in the IO data is the influence of the cerebellar cortex. The projection from the spinal trigeminal nucleus to IO is a major input to the cerebellum that plays a pivotal role in motor learning [144, 167-169] [170]. The magnocellular red nucleus projects directly to motoneurons and interneurons in the spinal cord, whereas the parvocellular red nucleus projects to the IO [171]. The effect of c-Fos neuronal activation within this brain region during motor learning may lie within this feedback loop. The mechanism of exactly how and what is happening during HFS or No-HFS treatment is unclear. If the neurons in the spinal trigeminal nucleus are projecting to same population of neurons in the IO that are receiving GABAergic input from the cerebellar nuclei, then IO activation may show no significant difference.

c- Fos Neuronal Activation in the Red Nucleus

The last region examined was the red nucleus during HFS and No-HFS stimulation. c-Fos labeled cells in the red nucleus were quantified because the contralateral red nucleus receives input from the ipsilateral interpositus neurons in the cerebellum and the red nucleus is the relay center for the sensorimotor cortex and the cerebellum [114, 172, 173] [174] [175]. The data demonstrated that rats with large gain changes showed significantly more c-Fos neuronal activation than rats with small gain changes in the contralateral red nucleus. More data is needed to conclude if other regions may affect the c-Fos activated cells within the contralateral RN. Nevertheless, it was shown that every major cortical area projects to the red nucleus and brain stem in the monkey [94] [176]. The present red nucleus data followed a similar trend as the spinal trigeminal nucleus and IO data for HFS and No-HFS conditions; the larger the gain changes the more c-Fos labeled cells. When HFS or any stimulation occurs, the trigeminal reflex circuit is being activated, but it is possible other brain regions may become activated and this may influence my data because the brain is interconnected. Based on previous data on trigeminal excitability [20] [99] and the current gain change data, c-Fos labeled neurons in the entire, anterior and posterior spinal trigeminal nucleus increase with the change in excitability. The trigeminal system becomes more excitable as the change in excitability from pre to post amplitude increases. The gain change showed a significant correlation with the change in excitability.

Overall, these experiments have provided significant implications for our understanding about neuronal activation in the trigeminal blink reflex during HFS modification. The HFS or No-HFS training did not affect the number of cells activated in the different regions of the trigeminal blink reflex circuit. The critical component was the gain change. These data suggested that the more suppressed the blink circuit, the more cells in the trigeminal become activated regardless of the condition. This is important when

we consider other regions in the brain sending inputs and outputs during these modifications and how the spinal trigeminal nucleus may be driving the inhibition in the trigeminal reflex blink.

Future experiments

In my study I focused on c-Fos activation in spinal trigeminal nucleus, inferior olive and red nucleus. It would be important to determine if the c-Fos cells activated in the regions previously mentioned along with cerebellum are inhibitory. To conduct these experiments, double labeling with c-Fos and GAD67/GlyT2 mRNA probes are crucial.

In PD blink modification is disrupted. Therefore c-Fos activation within trigeminal reflex circuit during HFS modification may provide insight about how neuronal expression is affected in a pathological state. The next set of experiments is, to compare c-Fos activation in spinal trigeminal nucleus, inferior olive, red nucleus and cerebellum of normal rats to 6-OHDA rat model of PD. These experiments will allow us to compare how active the neurons in interpositus are during HFS learning and single SO stimulation.

Labeling Inhibitory Neurons in Trigeminal Reflex Blink Circuit

The first experiment would be to utilize the doubling staining technique. A fluorescent *in situ* hybridization with GAD mRNA and GlyT2 probes combine with fluorescent *in situ* hybridization for c-Fos. A previous study showed that most of the inhibitory neurons in the sensory trigeminal might be both GABAergic and glycinergic [157]. First, the authors classified immunoreactive (ir) cells for GABA or glycine within the three subnuclei using GAD67 and GlyT2 probes. The results showed that neurons within spinal trigeminal nucleus coexpress GABA and glycine. Secondly one-third of neurons in caudalis region of the spinal trigeminal nucleus exhibited the most immunoreactive cells for both GABA and glycine followed by the interpolaris region. Nevertheless, Glutamic acid decarboxylase (GAD) is an enzyme that

synthesizes GABA that plays an important role in the nervous system. There are two forms of GAD, GAD65 and GAD67, each encoded by a different gene [177-180]. The two isoforms suggest that they may have different functional roles in the central nervous system. Previous studies showed that GAD65 and GAD67 are present in the same population of GABA neurons but differed in the quantity [177, 181-183]. GAD65 localized predominantly in the axon terminals, whereas GAD67 is found in the cell bodies[184]. GAD67 would be best in these experiments because labeling the cell bodies may inform us about the localization

of the cells present in the trigeminal blink circuit. On the other hand, the glycine transporter, GlyT2 is a specific and reliable marker for glycine immunoreactive neurons [185] [186] [187]. The first goal is to utilize the doubling staining technique using, GAD67 mRNA and GlyT2 with c-Fos staining for the spinal trigeminal nucleus, inferior olive, red nucleus and cerebellum. These experiments will help us to compare and identify GABA cells during HFS learning and single SO stimulation. Secondly, we can compare and quantify the amount of cells in ipsilateral and contralateral side of each brain region. Next we can utilize c-Fos neuronal activation as a function of gain change, to determine if more cells or less are activated with a larger gain change.

c-Fos Neuronal Activation in Rat Model of PD

The next experiment will include a 6-OHDA lesion rat model of PD. It was previously demonstrated that 6-OHDA lesion rats have impaired learning when undergoing the HFS-B paradigm [139]. Applying the HFS-B to rats and then double staining with c-Fos and GAD67 in the spinal trigeminal nucleus, inferior olive, red nucleus and cerebellum may provide insight about the impaired learning in these rats. It will also provide an understanding about how neuronal activity may be affected in each brain region due to the lack of dopamine. We can compare the percentage of labeled cells on ipsilateral and contralateral

side of unilateral 6-OHDA lesion rats. We can then compare neuronal activation during motor learning in normal rats and 6-OHDA lesion rats.

Recording from Right and Left Orbicularis Oculi

Lastly, in the present study I stimulated the left supraorbital nerve and recorded from the left orbicularis. In the above experiments stimulating the left supraorbital nerve and recording from the right and left orbicularis oculi may inform us how active is the side of the brain that is receiving stimulation compared to unstimulated side. Because in a previous study by Mao and Evinger, (2001) showed first, activating the SO that received HFS-B training produced a reduction in gain blinks in both the left and right eyelids. Secondly, activating the SO that did not receive HFS-B produced normal gain blinks in the left and right eyelids [107]. In summary these experiments may further elucidate our understanding about the trigeminal reflex blink circuit in normal and PD states.

Bibliography

[1] F. Battaglia, M.F. Ghilardi, A. Quartarone, S. Bagnato, P. Girlanda, M. Hallett, Impaired long-term potentiation-like plasticity of the trigeminal blink reflex circuit in Parkinson's disease, Movement disorders : official journal of the Movement Disorder Society, 21 (2006) 2230-2233.

[2] J. Kaminer, P. Thakur, C. Evinger, Effects of subthalamic deep brain stimulation on blink abnormalities of 6-OHDA lesioned rats, Journal of neurophysiology, 113 (2015) 3038-3046.

[3] A. Quartarone, A. Sant'Angelo, F. Battaglia, S. Bagnato, V. Rizzo, F. Morgante, J.C. Rothwell, H.R. Siebner, P. Girlanda, Enhanced long-term potentiation-like plasticity of the trigeminal blink reflex circuit in blepharospasm, The Journal of neuroscience : the official journal of the Society for Neuroscience, 26 (2006) 716-721.

[4] C. Evinger, M.D. Shaw, C.K. Peck, K.A. Manning, R. Baker, Blinking and associated eye movements in humans, guinea pigs, and rabbits, Journal of neurophysiology, 52 (1984) 323-339.

[5] D. Sevel, The origins and insertions of the extraocular muscles: development, histologic features, and clinical significance, Transactions of the American Ophthalmological Society, 84 (1986) 488-526.

[6] R.F. Spencer, J.D. Porter, Biological organization of the extraocular muscles, Progress in brain research, 151 (2006) 43-80.

[7] C. Beard, Muller's superior tarsal muscle: anatomy, physiology, and clinical significance, Ann Plast Surg, 14 (1985) 324-333.

[8] C. Evinger, K.A. Manning, P.A. Sibony, Eyelid movements. Mechanisms and normal data, Investigative ophthalmology & visual science, 32 (1991) 387-400.

[9] P.A. Sibony, C. Evinger, K.A. Manning, Eyelid movements in facial paralysis, Archives of ophthalmology, 109 (1991) 1555-1561.

[10] M.J. Doughty, Consideration of three types of spontaneous eyeblink activity in normal humans: during reading and video display terminal use, in primary gaze, and while in conversation, Optometry and vision science : official publication of the American Academy of Optometry, 78 (2001) 712-725.

[11] J. Kaminer, A.S. Powers, K.G. Horn, C. Hui, C. Evinger, Characterizing the spontaneous blink generator: an animal model, The Journal of neuroscience : the official journal of the Society for Neuroscience, 31 (2011) 11256-11267.

[12] J.A. Stern, L.C. Walrath, R. Goldstein, The endogenous eyeblink, Psychophysiology, 21 (1984) 22-33.

[13] C.N. Karson, Physiology of normal and abnormal blinking, Advances in neurology, 49 (1988) 25-37.

[14] T. Naase, M.J. Doughty, N.F. Button, An assessment of the pattern of spontaneous eyeblink activity under the influence of topical ocular anaesthesia, Graefe's archive for clinical and experimental ophthalmology = Albrecht von Graefes Archiv fur klinische und experimentelle Ophthalmologie, 243 (2005) 306-312.

[15] L.N. Orchard, J.A. Stern, Blinks as an index of cognitive activity during reading, Integrative physiological and behavioral science : the official journal of the Pavlovian Society, 26 (1991) 108-116.

[16] J.R. Taylor, J.D. Elsworth, M.S. Lawrence, J.R. Sladek, Jr., R.H. Roth, D.E. Redmond, Jr., Spontaneous blink rates correlate with dopamine levels in the caudate nucleus of MPTP-treated monkeys, Experimental neurology, 158 (1999) 214-220.

[17] M. Bologna, A. Fasano, N. Modugno, G. Fabbrini, A. Berardelli, Effects of subthalamic nucleus deep brain stimulation and L-DOPA on blinking in Parkinson's disease, Experimental neurology, 235 (2012) 265-272.

[18] M.S. Kleven, W. Koek, Differential effects of direct and indirect dopamine agonists on eye blink rate in cynomolgus monkeys, The Journal of pharmacology and experimental therapeutics, 279 (1996) 1211-1219.

[19] J.J. Pellegrini, A.K. Horn, C. Evinger, The trigeminally evoked blink reflex. I. Neuronal circuits, Experimental brain research, 107 (1995) 166-180.

[20] M.A. Basso, R.E. Strecker, C. Evinger, Midbrain 6-hydroxydopamine lesions modulate blink reflex excitability, Experimental brain research, 94 (1993) 88-96.

[21] E. Kugelberg, [Facial reflexes], Brain : a journal of neurology, 75 (1952) 385-396.

[22] B.J. Snow, R.W. Frith, The relationship of eyelid movement to the blink reflex, Journal of the neurological sciences, 91 (1989) 179-189.

[23] B.T. Shahani, R.R. Young, Human orbicularis oculi reflexes, Neurology, 22 (1972) 149-154.

[24] C. Lindquist, A. Martensson, Mechanisms involved in the cat's blink reflex, Acta physiologica Scandinavica, 80 (1970) 149-159.

[25] S. Anor, J.M. Espadaler, L. Monreal, I.G. Mayhew, Electrically induced blink reflex in horses, The Veterinary record, 139 (1996) 621-624.

[26] S. Anor, J.M. Espadaler, J. Pastor, M. Pumarola, Electrically induced blink reflex and facial motor nerve stimulation in beagles, Journal of veterinary internal medicine / American College of Veterinary Internal Medicine, 14 (2000) 418-423.

[27] B. Soliven, J. Meer, A. Uncini, J. Petajan, R. Lovelace, Physiologic and anatomic basis for contralateral R1 in blink reflex, Muscle & nerve, 11 (1988) 848-851.

[28] M. Trontelj, J.V. Trontelj, First component of human blink reflex studied on single facial motoneurones, Brain research, 53 (1973) 214-217.

[29] J.N. Sanes, J.A. Foss, J.R. Ison, Conditions that affect the thresholds of the components of the eyeblink reflex in humans, Journal of neurology, neurosurgery, and psychiatry, 45 (1982) 543-549.

[30] H.K. Walker, Cranial Nerve V: The Trigeminal Nerve, in: H.K. Walker, W.D. Hall, J.W. Hurst (Eds.) Clinical Methods: The History, Physical, and Laboratory Examinations, Boston, 1990.

[31] S. Gong, Q. Zhou, M.S. LeDoux, Blink-related sensorimotor anatomy in the rat, Anatomy and embryology, 207 (2003) 193-208.

[32] C.F. Marfurt, The central projections of trigeminal primary afferent neurons in the cat as determined by the tranganglionic transport of horseradish peroxidase, The Journal of comparative neurology, 203 (1981) 785-798.

[33] W.M. Panneton, H. Burton, Corneal and periocular representation within the trigeminal sensory complex in the cat studied with transganglionic transport of horseradish peroxidase, The Journal of comparative neurology, 199 (1981) 327-344.

[34] Y. Shigenaga, I.C. Chen, S. Suemune, T. Nishimori, I.D. Nasution, A. Yoshida, H. Sato, T. Okamoto, M. Sera, M. Hosoi, Oral and facial representation within the medullary and upper cervical dorsal horns in the cat, The Journal of comparative neurology, 243 (1986) 388-408.

[35] Y. Shigenaga, T. Okamoto, T. Nishimori, S. Suemune, I.D. Nasution, I.C. Chen, K. Tsuru, A. Yoshida, K. Tabuchi, M. Hosoi, et al., Oral and facial representation in the trigeminal principal and rostral spinal nuclei of the cat, The Journal of comparative neurology, 244 (1986) 1-18.

[36] J. Olszewski, On the anatomical and functional organization of the spinal trigeminal nucleus, The Journal of comparative neurology, 92 (1950) 401-413.

[37] Y. Shigenaga, K. Otani, S. Suemune, Morphology of central terminations of low-threshold trigeminal primary afferents from facial skin in the cat--intra-axonal staining with HRP, Brain research, 523 (1990) 23-50.

[38] R.D. Hall, B.L. Hicks, Two somatic eyelid reflexes in the albino rat, Physiology & behavior, 11 (1973) 167-176.

[39] M.D. Shaw, R. Baker, Morphology of motoneurons in a mixed motor pool of the cat facial nucleus that innervate orbicularis oculis and quadratus labii superioris, stained intracellularly with horseradish peroxidase, Neuroscience, 14 (1985) 627-643.

[40] J.D. Porter, L.A. Burns, P.J. May, Morphological substrate for eyelid movements: innervation and structure of primate levator palpebrae superioris and orbicularis oculi muscles, The Journal of comparative neurology, 287 (1989) 64-81.

[41] C.F. Hinrichsen, C.D. Watson, The facial nucleus of the rat: representation of facial muscles revealed by retrograde transport of horseradish peroxidase, The Anatomical record, 209 (1984) 407-415.

[42] B. Faulkner, T.H. Brown, C. Evinger, Identification and characterization of rat orbicularis oculi motoneurons using confocal laser scanning microscopy, Experimental brain research, 116 (1997) 10-19.

[43] R. Dengler, F. Rechl, A. Struppler, Recruitment of single motor units in the human blink reflex, Neuroscience letters, 34 (1982) 301-305.

[44] A. Gruart, B.G. Schreurs, E.D. del Toro, J.M. Delgado-Garcia, Kinetic and frequency-domain properties of reflex and conditioned eyelid responses in the rabbit, Journal of neurophysiology, 83 (2000) 836-852.

[45] C. Evinger, P.A. Sibony, K.A. Manning, R.A. Fiero, A pharmacological distinction between the long and short latency pathways of the human blink reflex revealed with tobacco, Experimental brain research, 73 (1988) 477-480.

[46] J. Kimura, Electrically elicited blink reflex in diagnosis of multiple sclerosis. Review of 260 patients over a seven-year period, Brain : a journal of neurology, 98 (1975) 413-426.

[47] L. Kiers, W.M. Carroll, Blink reflexes and magnetic resonance imaging in focal unilateral central trigeminal pathway demyelination, Journal of neurology, neurosurgery, and psychiatry, 53 (1990) 526-529.

[48] J.J. van Ham, C.H. Yeo, Trigeminal inputs to eyeblink motoneurons in the rabbit, Experimental neurology, 142 (1996) 244-257.

[49] G. Holstege, J.J. van Ham, J. Tan, Afferent projections to the orbicularis oculi motoneuronal cell group. An autoradiographical tracing study in the cat, Brain research, 374 (1986) 306-320.

[50] R.S. Erzurumlu, H.P. Killackey, Efferent connections of the brainstem trigeminal complex with the facial nucleus of the rat, The Journal of comparative neurology, 188 (1979) 75-86.

[51] V.M. Henriquez, C. Evinger, The three-neuron corneal reflex circuit and modulation of second-order corneal responsive neurons, Experimental brain research, 179 (2007) 691-702.

[52] M. Hiraoka, M. Shimamura, Neural mechanisms of the corneal blinking reflex in cats, Brain research, 125 (1977) 265-275.

[53] M. Inagaki, K. Takeshita, S. Nakao, Y. Shiraishi, T. Oikawa, An electrophysiologically defined trigemino-reticulo-facial pathway related to the blink reflex in the cat, Neuroscience letters, 96 (1989) 64-69.

[54] J.J. Van Ham, C.H. Yeo, Somatosensory Trigeminal Projections to the Inferior Olive, Cerebellum and other Precerebellar Nuclei in Rabbits, The European journal of neuroscience, 4 (1992) 302-317.

[55] M.F. Huerta, T. Hashikawa, M.J. Gayoso, J.K. Harting, The trigemino-olivary projection in the cat: contributions of individual subnuclei, The Journal of comparative neurology, 241 (1985) 180-190.

[56] N. Yatim, I. Billig, C. Compoint, P. Buisseret, C. Buisseret-Delmas, Trigeminocerebellar and trigemino-olivary projections in rats, Neuroscience research, 25 (1996) 267-283.

[57] M.F. Huerta, A. Frankfurter, J.K. Harting, Studies of the principal sensory and spinal trigeminal nuclei of the rat: projections to the superior colliculus, inferior olive, and cerebellum, The Journal of comparative neurology, 220 (1983) 147-167.

[58] F.W. Cody, H.C. Richardson, Responses of cerebellar interpositus nuclear neurones to trigeminal inputs in the cat [proceedings], The Journal of physiology, 277 (1978) 62P-63P.

[59] F.W. Cody, H.C. Richardson, Mossy and climbing fibre projections of trigeminal inputs to the cerebellar cortex in the cat, Brain research, 153 (1978) 352-356.

[60] F.W. Cody, H.C. Richardson, Trigeminal projections to the cerebellar cortex in the cat [proceedings], The Journal of physiology, 267 (1977) 41P-42P.

[61] A. Ndiaye, G. Pinganaud, C. Buisseret-Delmas, P. Buisseret, F. Vanderwerf, Organization of trigeminocollicular connections and their relations to the sensory innervation of the eyelids in the rat, The Journal of comparative neurology, 448 (2002) 373-387.

[62] T.J. Ruigrok, J. Voogd, Organization of projections from the inferior olive to the cerebellar nuclei in the rat, The Journal of comparative neurology, 426 (2000) 209-228.

[63] H.J. Groenewegen, J. Voogd, S.L. Freedman, The parasagittal zonation within the olivocerebellar projection. II. Climbing fiber distribution in the intermediate and hemispheric parts of cat cerebellum, The Journal of comparative neurology, 183 (1979) 551-601.

[64] R.H. Whitworth, Jr., D.E. Haines, On the question of nomenclature of homologous subdivisions of the inferior olivary complex, Archives italiennes de biologie, 124 (1986) 271-317.

[65] G. Andersson, D.M. Armstrong, Complex spikes in Purkinje cells in the lateral vermis (b zone) of the cat cerebellum during locomotion, The Journal of physiology, 385 (1987) 107-134.

[66] B.B. Gould, Organization of afferents from the brain stem nuclei to the cerebellar cortex in the cat, Adv Anat Embryol Cell Biol, 62 (1980) v-viii, 1-90.

[67] C.R. Watson, R.C. Switzer, 3rd, Trigeminal projections to cerebellar tactile areas in the rat-origin mainly from n. interpolaris and n. principalis, Neuroscience letters, 10 (1978) 77-82.

[68] J. Courville, Somatotopical organization of the projection from the nucleus interpositus anterior of the cerebellum to the red nucleus. An experimental study in the cat with silver impregnation methods, Experimental brain research, 2 (1966) 191-215.

[69] F. Conde, Cerebellar projections to the red nucleus of the cat, Behavioural brain research, 28 (1988) 65-68.

[70] T.M. Teune, J. van der Burg, T.J. Ruigrok, Cerebellar projections to the red nucleus and inferior olive originate from separate populations of neurons in the rat: a non-fluorescent double labeling study, Brain research, 673 (1995) 313-319.

[71] S. Morcuende, J.M. Delgado-Garcia, G. Ugolini, Neuronal premotor networks involved in eyelid responses: retrograde transneuronal tracing with rabies virus from the orbicularis oculi muscle in the rat, The Journal of neuroscience : the official journal of the Society for Neuroscience, 22 (2002) 8808-8818.

[72] H. Liang, G. Paxinos, C. Watson, The red nucleus and the rubrospinal projection in the mouse, Brain structure & function, 217 (2012) 221-232.

[73] K.D. Davis, J.O. Dostrovsky, Modulatory influences of red nucleus stimulation on the somatosensory responses of cat trigeminal subnucleus oralis neurons, Experimental neurology, 91 (1986) 80-101.

[74] J.E. Martinez-Lopez, J.A. Moreno-Bravo, M.P. Madrigal, S. Martinez, E. Puelles, Red nucleus and rubrospinal tract disorganization in the absence of Pou4f1, Front Neuroanat, 9 (2015) 8.

[75] R. Nyberg-Hansen, Functional organization of descending supraspinal fibre systems to the spinalcord. Anatomical observations and physiological correlations, Ergebnisse der Anatomie und Entwicklungsgeschichte, 39 (1966) 3-48.

[76] R. Nyberg-Hansen, A. Brodal, Sites and Mode of Termination of Rubrospinal Fibres in the Cat. An Experimental Study with Silver Impregnation Methods, Journal of anatomy, 98 (1964) 235-253.

[77] J.M. Wild, J.B. Cabot, D.H. Cohen, H.J. Karten, Origin, course and terminations of the rubrospinal tract in the pigeon (Columba livia), The Journal of comparative neurology, 187 (1979) 639-654.

[78] G. Warner, C.R. Watson, The rubrospinal tract in a diprotodont marsupial (Trichosurus vulpecula), Brain research, 41 (1972) 180-183.

[79] G. Holstege, Anatomical evidence for an ipsilateral rubrospinal pathway and for direct rubrospinal projections to motoneurons in the cat, Neuroscience letters, 74 (1987) 269-274.

[80] G. Holstege, B.F. Blok, D.D. Ralston, Anatomical evidence for red nucleus projections to motoneuronal cell groups in the spinal cord of the monkey, Neuroscience letters, 95 (1988) 97-101.

[81] M. Kuchler, K. Fouad, O. Weinmann, M.E. Schwab, O. Raineteau, Red nucleus projections to distinct motor neuron pools in the rat spinal cord, The Journal of comparative neurology, 448 (2002) 349-359.

[82] Y. Shinoda, C. Ghez, A. Arnold, Spinal branching of rubrospinal axons in the cat, Experimental brain research, 30 (1977) 203-218.

[83] Y. Shinoda, J. Yokota, T. Futami, Morphology of physiologically identified rubrospinal axons in the spinal cord of the cat, Brain research, 242 (1982) 321-325.

[84] R. Bandler, Evidence for a bilateral 'glomerular' projection from the red nucleus to the spinal nucleus of the trigeminal nerve in the cat, Neuroscience letters, 8 (1978) 211-217.

[85] S.B. Edwards, The ascending and descending projections of the red nucleus in the cat: an experimental study using an autoradiographic tracing method, Brain research, 48 (1972) 45-63.

[86] P.G. Kostyuk, G.G. Skibo, An electron microscopic analysis of rubrospinal tract termination in the spinal cord of the cat, Brain research, 85 (1975) 511-516.
[87] G.F. Martin, R. Dom, Rubrobulbar projections of the opossum (Didelphis virginiana), The Journal of comparative neurology, 139 (1970) 199-214.

[88] G.F. Martin, R. Dom, S. Katz, J.S. King, The organization of projection neurons in the opossum red nucleus, Brain research, 78 (1974) 17-34.

[89] R.A. Miller, N.L. Strominger, Efferent connections of the red nucleus in the brainstem and spinal cord of the Rhesus monkey, The Journal of comparative neurology, 152 (1973) 327-345.

[90] C.F. Hinrichsen, C.D. Watson, Brain stem projections to the facial nucleus of the rat, Brain, behavior and evolution, 22 (1983) 153-163.

[91] I. Molenaar, A. Rustioni, H.G. Kuypers, The location of cells of origin of the fibers in the ventral and the lateral funiculus of the cat's lumbo-sacral cord, Brain research, 78 (1974) 239-254.

[92] N.L. Hayes, A. Rustioni, Descending projections from brainstem and sensorimotor cortex to spinal enlargements in the cat. Single and double retrograde tracer studies, Experimental brain research, 41 (1981) 89-107.

[93] P. Sterling, H.G. Kuypers, Anatomical organization of the brachial spinal cord of the cat. 3. The propriospinal connections, Brain research, 7 (1968) 419-443.

[94] H.G. Kuypers, D.G. Lawrence, Cortical projections to the red nucleus and the brain stem in the Rhesus monkey, Brain research, 4 (1967) 151-188.

[95] H.G. Kuypers, V.A. Maisky, Retrograde axonal transport of horseradish peroxidase from spinal cord to brain stem cell groups in the cat, Neuroscience letters, 1 (1975) 9-14.

[96] B.G. Gray, J.O. Dostrovsky, Red nucleus modulation of somatosensory responses of cat spinal cord dorsal horn neurons, Brain research, 311 (1984) 171-175.

[97] U.C. Drager, D.H. Hubel, Physiology of visual cells in mouse superior colliculus and correlation with somatosensory and auditory input, Nature, 253 (1975) 203-204.

[98] J.K. Harting, R.W. Guillery, Organization of retinocollicular pathways in the cat, The Journal of comparative neurology, 166 (1976) 133-144.

[99] A.S. Powers, E.J. Schicatano, M.A. Basso, C. Evinger, To blink or not to blink: inhibition and facilitation of reflex blinks, Experimental brain research, 113 (1997) 283-290.

[100] J. Kimura, Disorder of interneurons in Parkinsonism. The orbicularis oculi reflex to paired stimuli, Brain : a journal of neurology, 96 (1973) 87-96.

[101] J.J. Pellegrini, C. Evinger, The trigeminally evoked blink reflex. II. Mechanisms of paired-stimulus suppression, Experimental brain research, 107 (1995) 181-196.

[102] M.A. Basso, A.S. Powers, C. Evinger, An explanation for reflex blink hyperexcitability in Parkinson's disease. I. Superior colliculus, The Journal of neuroscience : the official journal of the Society for Neuroscience, 16 (1996) 7308-7317.

[103] J.W. Gnadt, S.M. Lu, B. Breznen, M.A. Basso, V.M. Henriquez, C. Evinger, Influence of the superior colliculus on the primate blink reflex, Experimental brain research, 116 (1997) 389-398.

[104] M.A. Basso, C. Evinger, An explanation for reflex blink hyperexcitability in Parkinson's disease. II. Nucleus raphe magnus, The Journal of neuroscience : the official journal of the Society for Neuroscience, 16 (1996) 7318-7330.

[105] R. Agostino, A. Berardelli, G. Cruccu, F. Stocchi, M. Manfredi, Corneal and blink reflexes in Parkinson's disease with "on-off" fluctuations, Movement disorders : official journal of the Movement Disorder Society, 2 (1987) 227-235.

[106] E.J. Schicatano, K.R. Peshori, R. Gopalaswamy, E. Sahay, C. Evinger, Reflex excitability regulates prepulse inhibition, The Journal of neuroscience : the official journal of the Society for Neuroscience, 20 (2000) 4240-4247.

[107] J.B. Mao, C. Evinger, Long-term potentiation of the human blink reflex, The Journal of neuroscience : the official journal of the Society for Neuroscience, 21 (2001) RC151.

[108] M. Ryan, J. Kaminer, P. Enmore, C. Evinger, Trigeminal high-frequency stimulation produces short- and long-term modification of reflex blink gain, Journal of neurophysiology, 111 (2014) 888-895.

[109] D.A. McCormick, R.F. Thompson, Cerebellum: essential involvement in the classically conditioned eyelid response, Science, 223 (1984) 296-299.

[110] C.I. De Zeeuw, C.H. Yeo, Time and tide in cerebellar memory formation, Current opinion in neurobiology, 15 (2005) 667-674.

[111] H. Topka, J. Valls-Sole, S.G. Massaquoi, M. Hallett, Deficit in classical conditioning in patients with cerebellar degeneration, Brain : a journal of neurology, 116 (Pt 4) (1993) 961-969.

[112] K.M. Christian, R.F. Thompson, Neural substrates of eyeblink conditioning: acquisition and retention, Learning & memory, 10 (2003) 427-455.

[113] F.P. Chen, C. Evinger, Cerebellar modulation of trigeminal reflex blinks: interpositus neurons, The Journal of neuroscience : the official journal of the Society for Neuroscience, 26 (2006) 10569-10576.

[114] J.H. Freeman, A.B. Steinmetz, Neural circuitry and plasticity mechanisms underlying delay eyeblink conditioning, Learning & memory, 18 (2011) 666-677.

[115] D.A. Robinson, Adaptive gain control of vestibuloocular reflex by the cerebellum, Journal of neurophysiology, 39 (1976) 954-969.

[116] R.W. Baloh, R.D. Yee, J. Kimm, V. Honrubia, Vestibular-ocular reflex patients with lesions involving the vestibulocerebellum, Experimental neurology, 72 (1981) 141-152.

[117] L.M. Optican, D.A. Robinson, Cerebellar-dependent adaptive control of primate saccadic system, Journal of neurophysiology, 44 (1980) 1058-1076.

[118] A. Straube, W. Scheuerer, F.R. Robinson, T. Eggert, Temporary lesions of the caudal deep cerebellar nucleus in nonhuman primates. Gain, offset, and ocular alignment, Ann N Y Acad Sci, 1164 (2009) 119-126.

[119] J.J. Pellegrini, C. Evinger, Role of cerebellum in adaptive modification of reflex blinks, Learning & memory, 4 (1997) 77-87.

[120] J.I. Morgan, T. Curran, Role of ion flux in the control of c-fos expression, Nature, 322 (1986) 552-555.

[121] J.I. Morgan, D.R. Cohen, J.L. Hempstead, T. Curran, Mapping patterns of c-fos expression in the central nervous system after seizure, Science, 237 (1987) 192-197.

[122] E. Mugnaini, A.S. Berrebi, J.I. Morgan, T. Curran, Fos-Like Immunoreactivity Induced by Seizure in Mice Is Specifically Associated With Euchromatin in Neurons, The European journal of neuroscience, 1 (1989) 46-52.

[123] G.E. Hoffman, M.S. Smith, J.G. Verbalis, c-Fos and related immediate early gene products as markers of activity in neuroendocrine systems, Front Neuroendocrinol, 14 (1993) 173-213.

[124] D. Menetrey, A. Gannon, J.D. Levine, A.I. Basbaum, Expression of c-fos protein in interneurons and projection neurons of the rat spinal cord in response to noxious somatic, articular, and visceral stimulation, The Journal of comparative neurology, 285 (1989) 177-195.

[125] S.P. Hunt, A. Pini, G. Evan, Induction of c-fos-like protein in spinal cord neurons following sensory stimulation, Nature, 328 (1987) 632-634.

[126] L.F. Lau, D. Nathans, Expression of a set of growth-related immediate early genes in BALB/c 3T3 cells: coordinate regulation with c-fos or c-myc, Proceedings of the National Academy of Sciences of the United States of America, 84 (1987) 1182-1186.

[127] K.J. Jones, C. Evinger, Differential neuronal expression of c-fos proto-oncogene following peripheral nerve injury or chemically-induced seizure, Journal of neuroscience research, 28 (1991) 291-298.

[128] R.M. Gubits, J.L. Hazelton, R. Simantov, Variations in c-fos gene expression during rat brain development, Brain research, 427 (1988) 197-201.

[129] R.M. Gubits, J.L. Fairhurst, c-fos mRNA levels are increased by the cellular stressors, heat shock and sodium arsenite, Oncogene, 3 (1988) 163-168.

[130] M. Dragunow, H.A. Robertson, Kindling stimulation induces c-fos protein(s) in granule cells of the rat dentate gyrus, Nature, 329 (1987) 441-442.

[131] M. Dragunow, H.A. Robertson, Generalized seizures induce c-fos protein(s) in mammalian neurons, Neuroscience letters, 82 (1987) 157-161.

[132] M. Dragunow, M.R. Peterson, H.A. Robertson, Presence of c-fos-like immunoreactivity in the adult rat brain, Eur J Pharmacol, 135 (1987) 113-114.

[133] S. Williams, G. Evan, S.P. Hunt, Spinal c-fos induction by sensory stimulation in neonatal rats, Neuroscience letters, 109 (1990) 309-314.

[134] E. Bullitt, Somatotopy of spinal nociceptive processing, The Journal of comparative neurology, 312 (1991) 279-290.

[135] Y.A. Berrocal, D.D. Pearse, C.M. Andrade, J.F. Hechtman, R. Puentes, M.J. Eaton, Increased spinal c-Fos expression with noxious and non-noxious peripheral stimulation after severe spinal contusion, Neuroscience letters, 413 (2007) 58-62.

[136] F. Zerari-Mailly, C. Dauvergne, P. Buisseret, C. Buisseret-Delmas, Localization of trigeminal, spinal, and reticular neurons involved in the rat blink reflex, The Journal of comparative neurology, 467 (2003) 173-184.

[137] C. Evinger, Eyelid Anatomy and the Pathophysiology of Blinking, Encyclopedia of the Eye, Oxford, 2010, pp. 128-133.

[138] J. Campellone, D. Zieve, Trigeminal Nerualigia, A.D.A.M Editorial team, 2014.

[139] J. Kaminer, P. Thakur, C. Evinger, Frequency matters: beta-band subthalamic nucleus deep-brain stimulation induces Parkinsonian-like blink abnormalities in normal rats, The European journal of neuroscience, 40 (2014) 3237-3242.

[140] G. Paxinos, C. Watson, The rat Brain in stereotaxic coordinates, Academic Press, San Diego, California, 1998.

[141] M.F. Jacquin, N.L. Chiaia, J.H. Haring, R.W. Rhoades, Intersubnuclear connections within the rat trigeminal brainstem complex, Somatosensory & motor research, 7 (1990) 399-420.

[142] J.J. Kim, D.J. Krupa, R.F. Thompson, Inhibitory cerebello-olivary projections and blocking effect in classical conditioning, Science, 279 (1998) 570-573.

[143] L.L. Sears, J.E. Steinmetz, Dorsal accessory inferior olive activity diminishes during acquisition of the rabbit classically conditioned eyelid response, Brain research, 545 (1991) 114-122.

[144] M.D. Mauk, J.E. Steinmetz, R.F. Thompson, Classical conditioning using stimulation of the inferior olive as the unconditioned stimulus, Proceedings of the National Academy of Sciences of the United States of America, 83 (1986) 5349-5353.

[145] K.J. Kovacs, Measurement of immediate-early gene activation- c-fos and beyond, Journal of neuroendocrinology, 20 (2008) 665-672.

[146] A.T. Konkle, C. Bielajew, Tracing the neuroanatomical profiles of reward pathways with markers of neuronal activation, Rev Neurosci, 15 (2004) 383-414.

[147] K. Deisseroth, S. Singla, H. Toda, M. Monje, T.D. Palmer, R.C. Malenka, Excitation-neurogenesis coupling in adult neural stem/progenitor cells, Neuron, 42 (2004) 535-552.

[148] M. Devor, R. Amir, Z.H. Rappaport, Pathophysiology of trigeminal neuralgia: the ignition hypothesis, Clin J Pain, 18 (2002) 4-13.

[149] B.W. Ongerboer de Visser, D. Moffie, Effects of brain-stem and thalamic lesions on the corneal reflex: an electrophysiological and anatomical study, Brain : a journal of neurology, 102 (1979) 595-608.

[150] C. Evinger, M.A. Basso, K.A. Manning, P.A. Sibony, J.J. Pellegrini, A.K. Horn, A role for the basal ganglia in nicotinic modulation of the blink reflex, Experimental brain research, 92 (1993) 507-515.

[151] M. Takemura, T. Sugimoto, Y. Shigenaga, Difference in central projection of primary afferents innervating facial and intraoral structures in the rat, Experimental neurology, 111 (1991) 324-331.

[152] C.F. Marfurt, D.R. Del Toro, Corneal sensory pathway in the rat: a horseradish peroxidase tracing study, The Journal of comparative neurology, 261 (1987) 450-459.

[153] V.M. Henriquez, C. Evinger, Modification of cornea-evoked reflex blinks in rats, Experimental brain research, 163 (2005) 445-456.

[154] H. Hirata, S. Takeshita, J.W. Hu, D.A. Bereiter, Cornea-responsive medullary dorsal horn neurons: modulation by local opioids and projections to thalamus and brain stem, Journal of neurophysiology, 84 (2000) 1050-1061.

[155] I.D. Meng, J.W. Hu, D.A. Bereiter, Differential effects of morphine on corneal-responsive neurons in rostral versus caudal regions of spinal trigeminal nucleus in the rat, Journal of neurophysiology, 79 (1998) 2593-2602.

[156] H. Hirata, K. Okamoto, D.A. Bereiter, GABA(A) receptor activation modulates corneal unit activity in rostral and caudal portions of trigeminal subnucleus caudalis, Journal of neurophysiology, 90 (2003) 2837-2849.

[157] C. Avendano, R. Machin, P.E. Bermejo, A. Lagares, Neuron numbers in the sensory trigeminal nuclei of the rat: A GABA- and glycine-immunocytochemical and stereological analysis, The Journal of comparative neurology, 493 (2005) 538-553.

[158] M.S. Bull, S.K. Mitchell, K.J. Berkley, Convergent inputs to the inferior olive from the dorsal column nuclei and pretectum in the cat, Brain research, 525 (1990) 1-10.

[159] E. Leznik, V. Makarenko, R. Llinas, Electrotonically mediated oscillatory patterns in neuronal ensembles: an in vitro voltage-dependent dye-imaging study in the inferior olive, The Journal of neuroscience : the official journal of the Society for Neuroscience, 22 (2002) 2804-2815.

[160] I. Lampl, Y. Yarom, Subthreshold oscillations and resonant behavior: two manifestations of the same mechanism, Neuroscience, 78 (1997) 325-341.

[161] M.A. Long, M.R. Deans, D.L. Paul, B.W. Connors, Rhythmicity without synchrony in the electrically uncoupled inferior olive, The Journal of neuroscience : the official journal of the Society for Neuroscience, 22 (2002) 10898-10905.

[162] L.S. Benardo, R.E. Foster, Oscillatory behavior in inferior olive neurons: mechanism, modulation, cell aggregates, Brain Res Bull, 17 (1986) 773-784.

[163] A.F. Bleasel, A.G. Pettigrew, Development and properties of spontaneous oscillations of the membrane potential in inferior olivary neurons in the rat, Brain Res Dev Brain Res, 65 (1992) 43-50.

[164] Y. Manor, J. Rinzel, I. Segev, Y. Yarom, Low-amplitude oscillations in the inferior olive: a model based on electrical coupling of neurons with heterogeneous channel densities, Journal of neurophysiology, 77 (1997) 2736-2752.

[165] Y. Loewenstein, Y. Yarom, H. Sompolinsky, The generation of oscillations in networks of electrically coupled cells, Proceedings of the National Academy of Sciences of the United States of America, 98 (2001) 8095-8100.

[166] K.J. Berkley, P.J. Hand, Projections to the inferior olive of the cat. II. Comparisons of input from the gracile, cuneate and the spinal trigeminal nuclei, The Journal of comparative neurology, 180 (1978) 253-264.

[167] R. Llinas, J.P. Welsh, On the cerebellum and motor learning, Current opinion in neurobiology, 3 (1993) 958-965.

[168] J.P. Welsh, J.A. Harvey, Acute inactivation of the inferior olive blocks associative learning, The European journal of neuroscience, 10 (1998) 3321-3332.

[169] M. Ito, Neural design of the cerebellar motor control system, Brain research, 40 (1972) 81-84.

[170] D. Marr, A theory of cerebellar cortex, The Journal of physiology, 202 (1969) 437-470.

[171] C.I. De Zeeuw, J.I. Simpson, C.C. Hoogenraad, N. Galjart, S.K. Koekkoek, T.J. Ruigrok, Microcircuitry and function of the inferior olive, Trends Neurosci, 21 (1998) 391-400.

[172] P.F. Chapman, J.E. Steinmetz, L.L. Sears, R.F. Thompson, Effects of lidocaine injection in the interpositus nucleus and red nucleus on conditioned behavioral and neuronal responses, Brain research, 537 (1990) 149-156.

[173] V. Bracha, S. Zbarska, K. Parker, A. Carrel, G. Zenitsky, J.R. Bloedel, The cerebellum and eye-blink conditioning: learning versus network performance hypotheses, Neuroscience, 162 (2009) 787-796.

[174] R.E. Clark, D.G. Lavond, Reversible lesions of the red nucleus during acquisition and retention of a classically conditioned behavior in rabbits, Behavioral neuroscience, 107 (1993) 264-270.

[175] J.E. Desmond, J.W. Moore, Single-unit activity in red nucleus during the classically conditioned rabbit nictitating membrane response, Neuroscience research, 10 (1991) 260-279.

[176] R.N. Lemon, Cortical projections to the red nucleus and the brain stem in the rhesus monkey, Brain research, 1645 (2016) 28-30.

[177] M.G. Erlander, N.J. Tillakaratne, S. Feldblum, N. Patel, A.J. Tobin, Two genes encode distinct glutamate decarboxylases, Neuron, 7 (1991) 91-100.

[178] M.G. Erlander, A.J. Tobin, The structural and functional heterogeneity of glutamic acid decarboxylase: a review, Neurochemical research, 16 (1991) 215-226.

[179] D.L. Martin, S.B. Martin, S.J. Wu, N. Espina, Cofactor interactions and the regulation of glutamate decarboxylase activity, Neurochemical research, 16 (1991) 243-249.

[180] D.L. Martin, S.B. Martin, S.J. Wu, N. Espina, Regulatory properties of brain glutamate decarboxylase (GAD): the apoenzyme of GAD is present principally as the smaller of two molecular forms of GAD in brain, The Journal of neuroscience : the official journal of the Society for Neuroscience, 11 (1991) 2725-2731.

[181] S. Feldblum, M.G. Erlander, A.J. Tobin, Different distributions of GAD65 and GAD67 mRNAs suggest that the two glutamate decarboxylases play distinctive functional roles, Journal of neuroscience research, 34 (1993) 689-706.

[182] M. Mercugliano, J.J. Soghomonian, Y. Qin, H.Q. Nguyen, S. Feldblum, M.G. Erlander, A.J. Tobin, M.F. Chesselet, Comparative distribution of messenger RNAs encoding glutamic acid decarboxylases (Mr 65,000 and Mr 67,000) in the basal ganglia of the rat, The Journal of comparative neurology, 318 (1992) 245-254.

[183] M. Esclapez, N.J. Tillakaratne, A.J. Tobin, C.R. Houser, Comparative localization of mRNAs encoding two forms of glutamic acid decarboxylase with nonradioactive in situ hybridization methods, The Journal of comparative neurology, 331 (1993) 339-362.

[184] D.L. Kaufman, C.R. Houser, A.J. Tobin, Two forms of the gamma-aminobutyric acid synthetic enzyme glutamate decarboxylase have distinct intraneuronal distributions and cofactor interactions, Journal of neurochemistry, 56 (1991) 720-723.

[185] I. Poyatos, J. Ponce, C. Aragon, C. Gimenez, F. Zafra, The glycine transporter GLYT2 is a reliable marker for glycine-immunoreactive neurons, Brain Res Mol Brain Res, 49 (1997) 63-70.

[186] M. Hossaini, L.S. Duraku, C. Sarac, J.L. Jongen, J.C. Holstege, Differential distribution of activated spinal neurons containing glycine and/or GABA and expressing c-fos in acute and chronic pain models, Pain, 151 (2010) 356-365.

[187] M. Hossaini, J.A. Goos, S.K. Kohli, J.C. Holstege, Distribution of glycine/GABA neurons in the ventromedial medulla with descending spinal projections and evidence for an ascending glycine/GABA projection, PLoS One, 7 (2012) e35293.